

# CHAPTER 2 LITERATURE REVIEW

## 2.1 Introduction

Polyimides are step or condensation polymers derived from both aliphatic or aromatic dianhydrides and diamines, or their derivatives, and contain a heterocyclic imide linkage in the repeat unit, as shown in Figure 2.1.

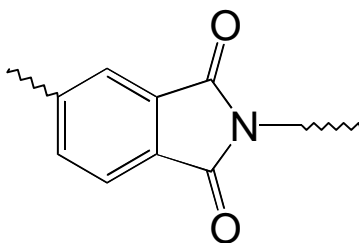


Figure 2.1 A Heterocyclic Imide Linkage

Polyimides are both scientifically and commercially important due to their excellent thermal stability and mechanical strength. Innovative polyimide design has led to their use in aerospace, microelectronics, automotive and packaging industries.

This chapter will discuss topics relevant to this dissertation, including synthetic chemistry, methods of polyimide preparation, polymer characterization, applications, gas separations theory, and structure/property relationships in gas permeation science.

## 2.2 Synthesis of Polyimides

The number of versatile synthetic methods for the formation of polyimides has facilitated their range of utility in high performance applications.<sup>1-9</sup> The prominent synthetic methods as well as some more novel routes to polyimide formation will be presented in this section.

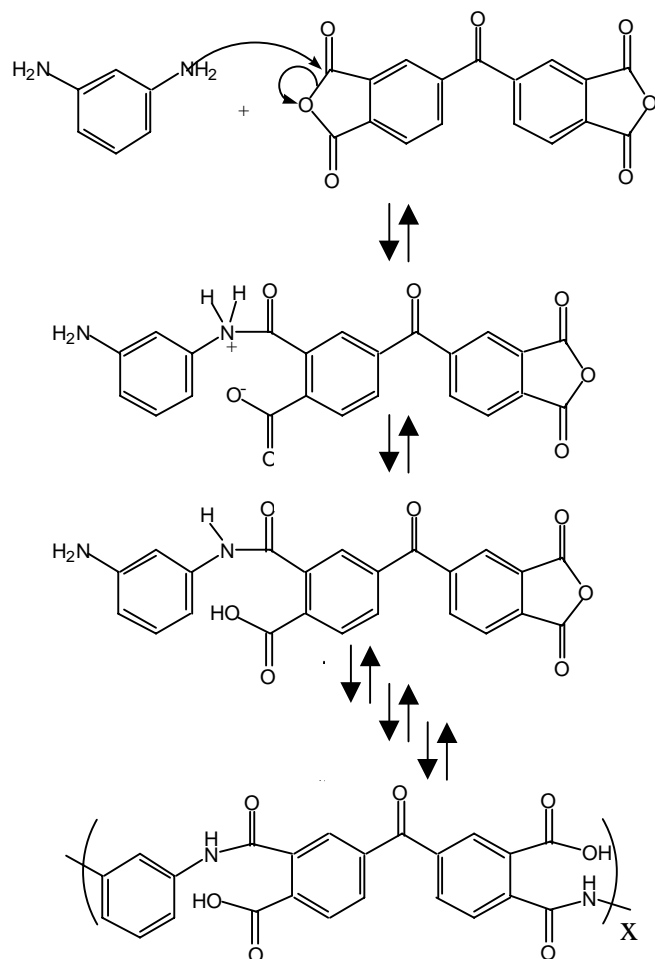
## 2.2.1 Classical Two-Step Method

### 2.2.1.1 Poly(amic acid) Formation

The most important method for polyimide synthesis has been the “two-step” method involving a polyamic acid (PAA) precursor, which is subsequently cyclized to form the imide linkage. This route is also known as the “classical” method. Many of the mechanistic pathways involved have been elucidated by a number of researchers over the past forty years.

Generally, the polyamic acid is formed when a difunctional amine and a difunctional anhydride mutually react in a polar aprotic solvent. This proceeds by a reversible nucleophilic substitution reaction when the amine attacks one of the carbonyl carbons in the anhydride moiety and displaces a carboxylate functionality, followed by proton transfer (Scheme 2.2.1.1.1). The reactivity and concentration of each of the monomeric units and the nature of the solvent will determine the rate of PAA formation and its stability with regard to other reagents.

Some typical dianhydrides and diamines are shown in Figure 2.2.1.1.1, along with their common acronyms. Dianhydride reactivity was found to best correlate with electron affinity ( $E_a$ ) (Table 2.2.1.1.1),<sup>10</sup> and thus, the dianhydride with the greatest electrophilicity, i.e. the highest electron affinity, will react first with a given nucleophile. As shown by  $E_a$  values in Table 2.2.1.1.1, PMDA is clearly much more reactive than the other anhydrides. The reason for the relatively high reactivity of PMDA and the range of dianhydride  $E_a$ s observed is the differences in electronic environment of the anhydride carbonyl groups which can easily be illustrated with BTDA, BPDA, and ODPA. BTDA is bridged by an electron withdrawing carbonyl group. By removing electron density through the pi-orbitals, the anhydride carbons experience a greater positive environment, which facilitate attack by a nucleophile. ODPA on the other hand is linked by an oxygen atom which is able to donate electrons into the ring thereby reducing the anhydride carbons' affinity for incoming electrons from an attacking nucleophile. In the case of BPDA, where no bridging functionality is present to either withdraw or donate electron density, an intermediate  $E_a$  value between BTDA and ODPA is observed.



Scheme 2.2.1.1.1 Isomeric Polyamic Acid Formation via Nucleophilic Substitution at an Anhydride Carbonyl

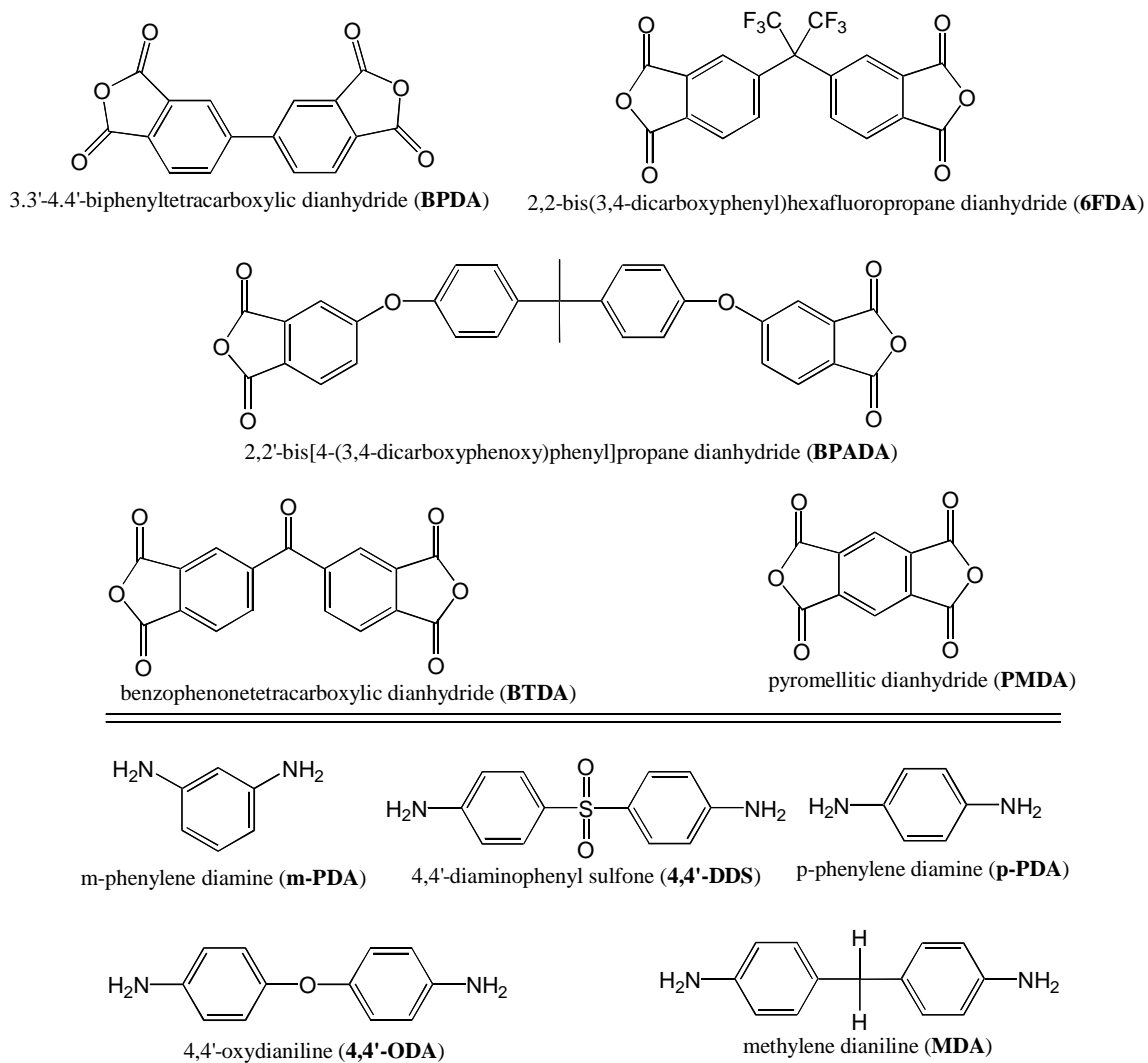
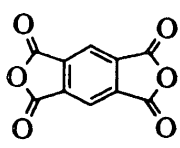
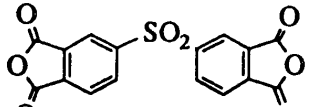
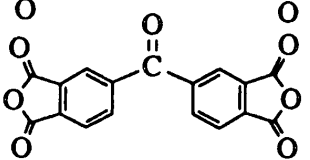
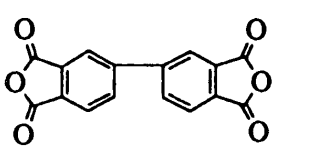
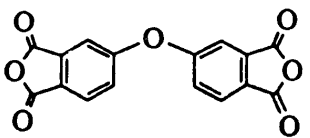
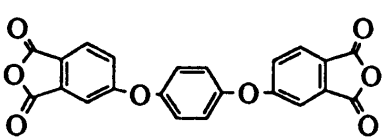
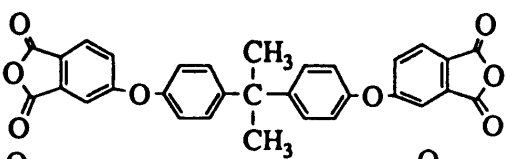
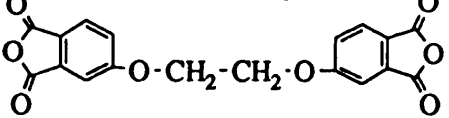


Figure 2.2.1.1.1 Common Dianhydrides and Diamines

Table 2.2.1.1.1 Electron Affinity of Representative Aromatic Dianhydrides<sup>10</sup>

Dianhydrides	$E_a$ (eV)
	<b>(PMDA)</b> 1.90
	<b>(DSDA)</b> 1.57
	<b>(BTDA)</b> 1.55
	<b>(BPDA)</b> 1.38
	<b>(ODPA)</b> 1.30
	<b>(HQDA)</b> 1.19
	<b>(BPADA)</b> 1.12
	<b>(EDA)</b> 1.10

It is also known that when electron withdrawing and donating bridges are present, they will have greater influence on  $E_a$  when located para- or ortho- to the anhydride carbonyls.

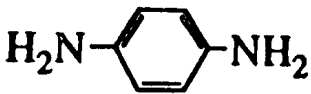
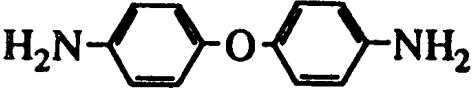
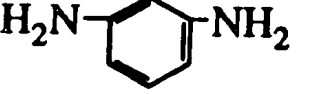
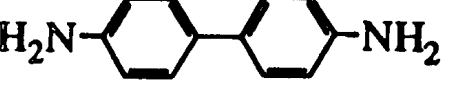
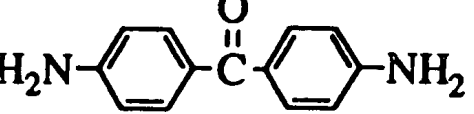
Diamine reactivity towards phthalic anhydride was found to correlate well with basicity  $pK_a$  (Table 2.2.1.1.2),<sup>11</sup> eg. an amine with a greater basicity will react faster. A diamine bridged by a withdrawing group, eg. diaminobenzophenone, shows decreased nucleophilicity.

When diamines and dianhydrides of low reactivity are used for PAA formation, a lower molecular weight would be expected when compared to a highly reactive diamine/dianhydride system,<sup>12</sup> assuming a fixed reaction time since  $X_n$  is directly dependent on  $1/(1-p)$  ( $p$  = degree of polymerization).

From the discussion above, it is already apparent that the rate of PAA formation is largely dependent on diamine basicity and anhydride electron affinity. However, reaction rate is also a function of the solvent. The overall reaction involves a relatively weak base reacting with a non-protic anhydride to yield a strong protic acid. In general, this reaction is enhanced when a more basic aprotic solvent is utilized<sup>13</sup> due to its favorable interaction with the strong acid (NMP>DMAc>acetonitrile>THF). In fact, it has been speculated by some that using a 4:1 ratio of DMAc or NMP allows complexation with each di(amic acid) repeat unit (Figure 2.2.1.1.2)<sup>14,15</sup>, which could be a driving force for PAA formation. However, if the aprotic solvent is not basic enough it is possible that the strong acid formed may autoaccelerate the reaction and also shift the equilibrium away from high molecular weight PAA.<sup>16</sup>

It has been reported that diamines which are weak bases, such as 4,4'-diaminodiphenylsulfones, react slowly with BTDA in DMAc, but high molecular weights are rapidly achieved in THF.<sup>17</sup> Two possible explanations for this are proposed. There may be a specific interaction between the amine and THF which increases its basicity and/or the THF may not be basic enough to deprotonate the acid to form the carboxylate, thus driving the reverse reaction.<sup>12</sup>

Table 2.2.1.1.2 Basicity  $pK_a$  of Diamines and Their Reactivity Towards 1,2,4,5-Benzenetetracarboxylic Dianhydride (PMDA)<sup>11</sup>

Diamine	$pK_a$	$\log k$
	6.08	2.12
	5.20	0.78
	4.80	0
	4.60	0.37
	3.10	-2.15

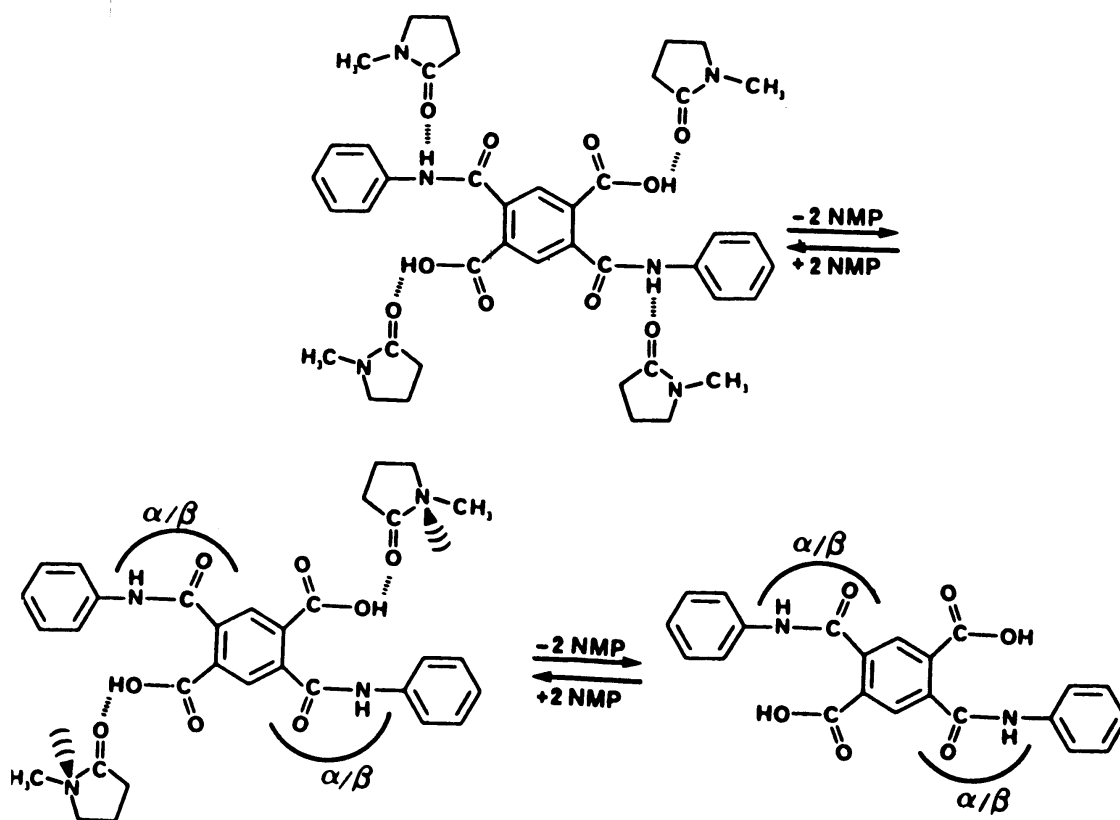


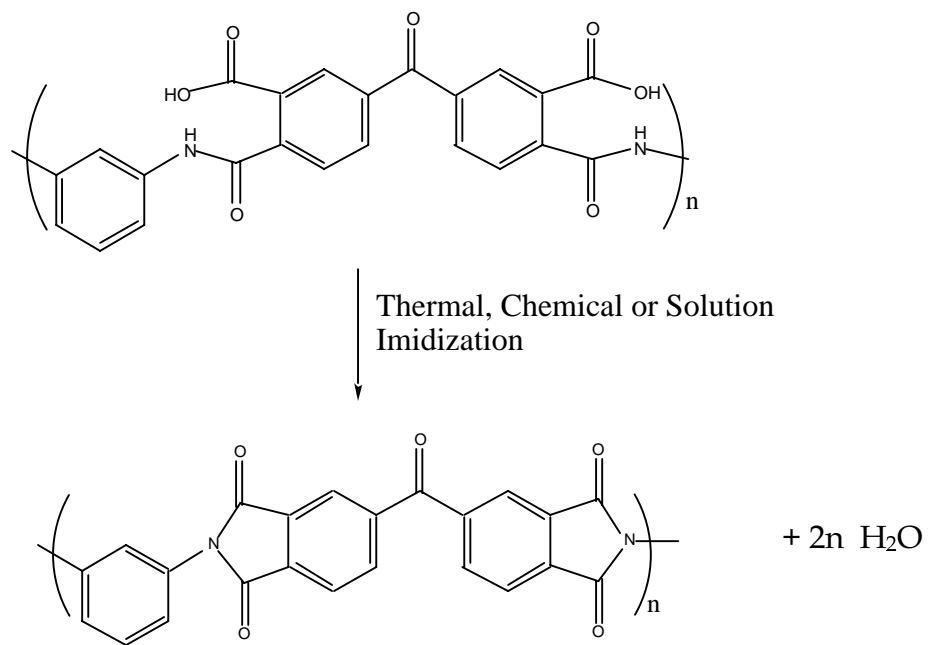
Figure 2.2.1.1.2 A Model for a 4:1 Ratio of NMP Complexation with a Di(amic acid) Repeat Unit<sup>15</sup>



To enable formation of PAA having a well-defined molecular weight, it is imperative to completely remove water from the monomers and the reaction solvents. This is usually achieved by carefully drying the monomers and distilling the solvents. In the presence of water the dianhydride will hydrolyze to form the diacid which reacts at a much slower rate with a given amine. Water will also promote the reverse reaction, which is hydrolytic scission of the amide link. Cyclization of PAA will also generate water and may facilitate chain hydrolysis. Three methods have been employed to facilitate the cyclization of PAA and the removal of water. Cyclization and the removal of water can be achieved by either heating the PAA in solution or as a cast film, or it can be chemically induced through the addition of dehydrating reagents (Scheme 2.2.1.1.2).

### ***2.2.1.2 Thermal (Bulk) Imidization***

Polyamic acids, which may precipitate upon cyclization due to the increase in chain rigidity, are generally cast from solution and thermally imidized in a film form, which is also known as “bulk imidization”. Commercial examples of polyimides produced by this route include the Kapton family from DuPont (Figure 2.2.1.2.1). A widely employed<sup>1</sup> laboratory thermal cycle, conducted under vacuum or nitrogen to remove water and prepare bubble-free films is as follows: R.T. for one hour, 100°C for one hour, 200°C for one hour, and 300°C for one hour. Important features of the solid-state imidization reaction are still incompletely understood, including the influence of decreased molecular mobility and the effect of residual solvent.<sup>18</sup> Although the mechanism is not well understood, it is thought to proceed by a nucleophilic substitution reaction involving the amide nitrogen and the ortho-carboxylic acid. The product of this reaction, water, is then thermally removed. This mechanism has been established for solution imidized systems and will be discussed later. The bulk reaction is known to be promoted by residual solvent. Not only does solvent plasticize the film, which allows greater chain mobility, but it also favors the appropriate conformation needed for cyclization to occur.<sup>14</sup> An increase in chain mobility



Scheme 2.2.1.1.2 Three Common Routes to Facilitate the Conversion of Polyamide Acids to Polyimides

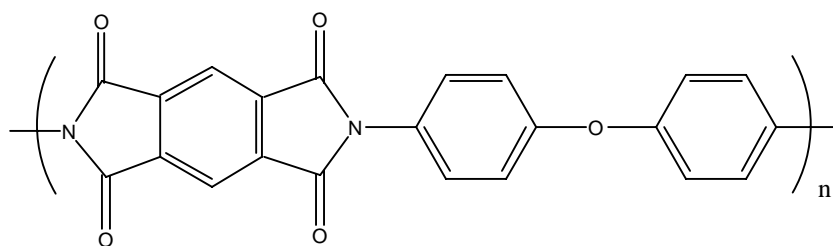


Figure 2.2.1.2.1 The Repeat Unit of Kapton-H Formed from PMDA and ODA<sup>19</sup>

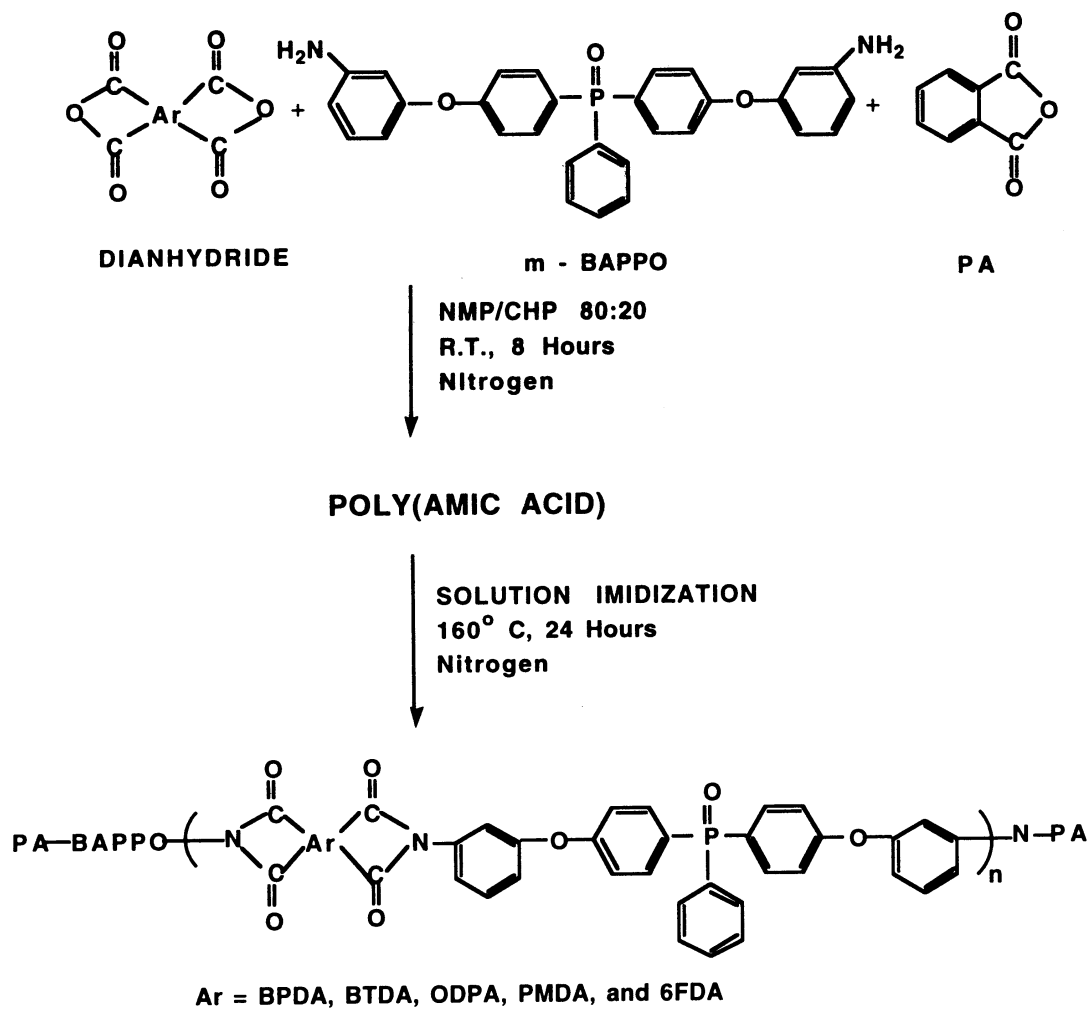
is required to fully cyclize the PAA. Chain mobility can also be achieved above the glass transition temperature of the polyimide.

### **2.2.1.3 Solution Imidization**

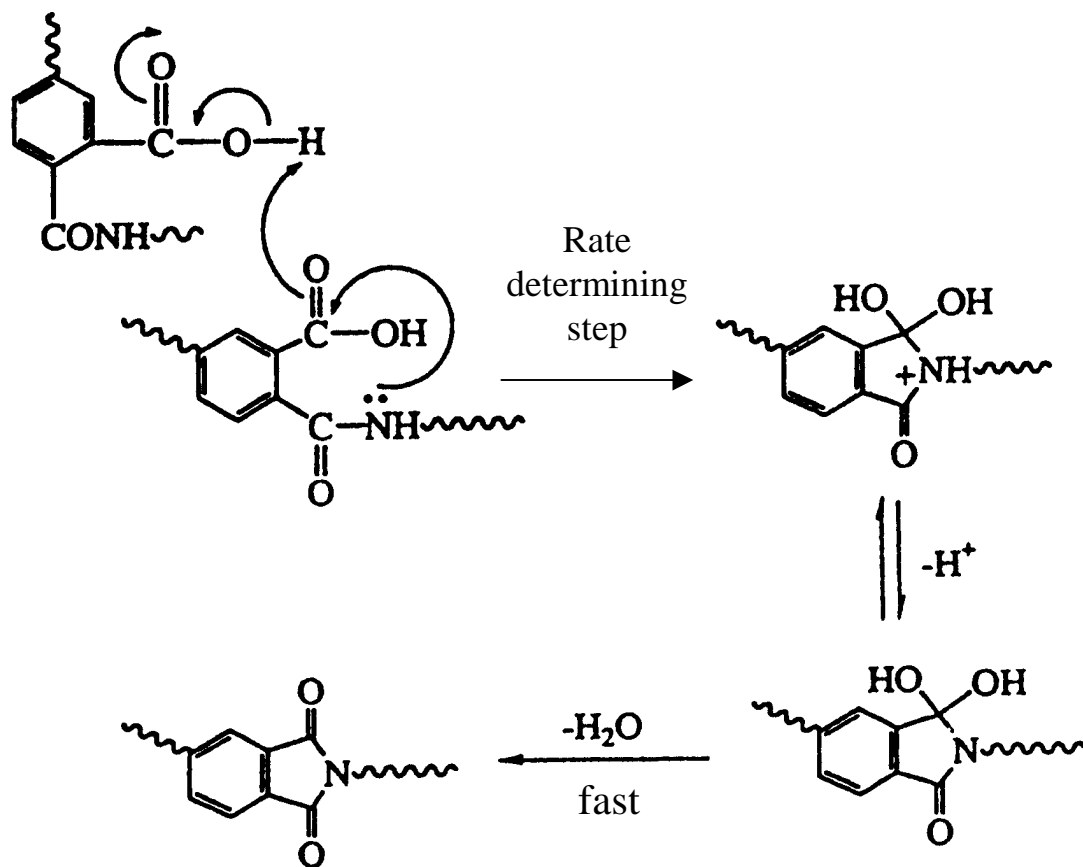
Polyimides which remain soluble in the fully cyclized form can be thermally imidized from the corresponding PAA's in solution at elevated temperatures. A typical solvent combination and temperature profile is shown in Scheme 2.2.1.3.1.<sup>20</sup> An azeotroping solvent is typically used in order to remove the water formed during the reaction to drive the reaction to completion. The solvent of choice needs to be capable of transporting the water from the reaction. Typical azeotroping solvents are: toluene, xylene, o-dichlorobenzene (o-DCB), or cyclohexyl pyrrolidone (CHP).

Kim et al. has recently proposed a reaction mechanism for the imidization of homogeneous systems in solution (Scheme 2.2.1.3.2).<sup>21</sup> The rate determining step in this process, which was recently confirmed by Furukawa et al.,<sup>22</sup> is second order with respect to PAA links and is also acid catalyzed. Imidization was also monitored by titration analysis as a function of temperature (Figure 2.2.1.3.1).<sup>21</sup> Initially, the viscosity of the PAA solution was high but as the reaction temperature increased, a dramatic decrease in the solution viscosity was observed. The drop in viscosity has also been noted by others during solution imidization.<sup>23-25</sup> The initial drop in viscosity could be interpreted as resulting from the following: a shift in the equilibrium from the PAA back to the free amine/anhydride and/or an acid-catalyzed hydrolysis of amide bonds.<sup>21</sup> In either case, the chain undergoes scission, which has been confirmed by <sup>1</sup>H NMR measurements. The subsequent viscosity build up is due to the restoration of long chains as scissioned units reunite and subsequently cyclodehydrate to form the high molecular weight polyimide.

Complete backbone cyclization, shown in Figure 2.2.1.3.1, occurred at 180°C within 12 hours. However, even after 24 hours at lower temperatures, eg. 140°C and 150°C, incomplete imidization was evident. It is well known that incomplete imidization will affect the end use properties because the residual amide linkages are readily



Scheme 2.2.1.3.1 Synthesis of m-BAPPO Based Polyimides via Solution Imidization<sup>20</sup>



Scheme 2.2.1.3.2 A Reaction Mechanism for the Solution Imidization Process<sup>21</sup>

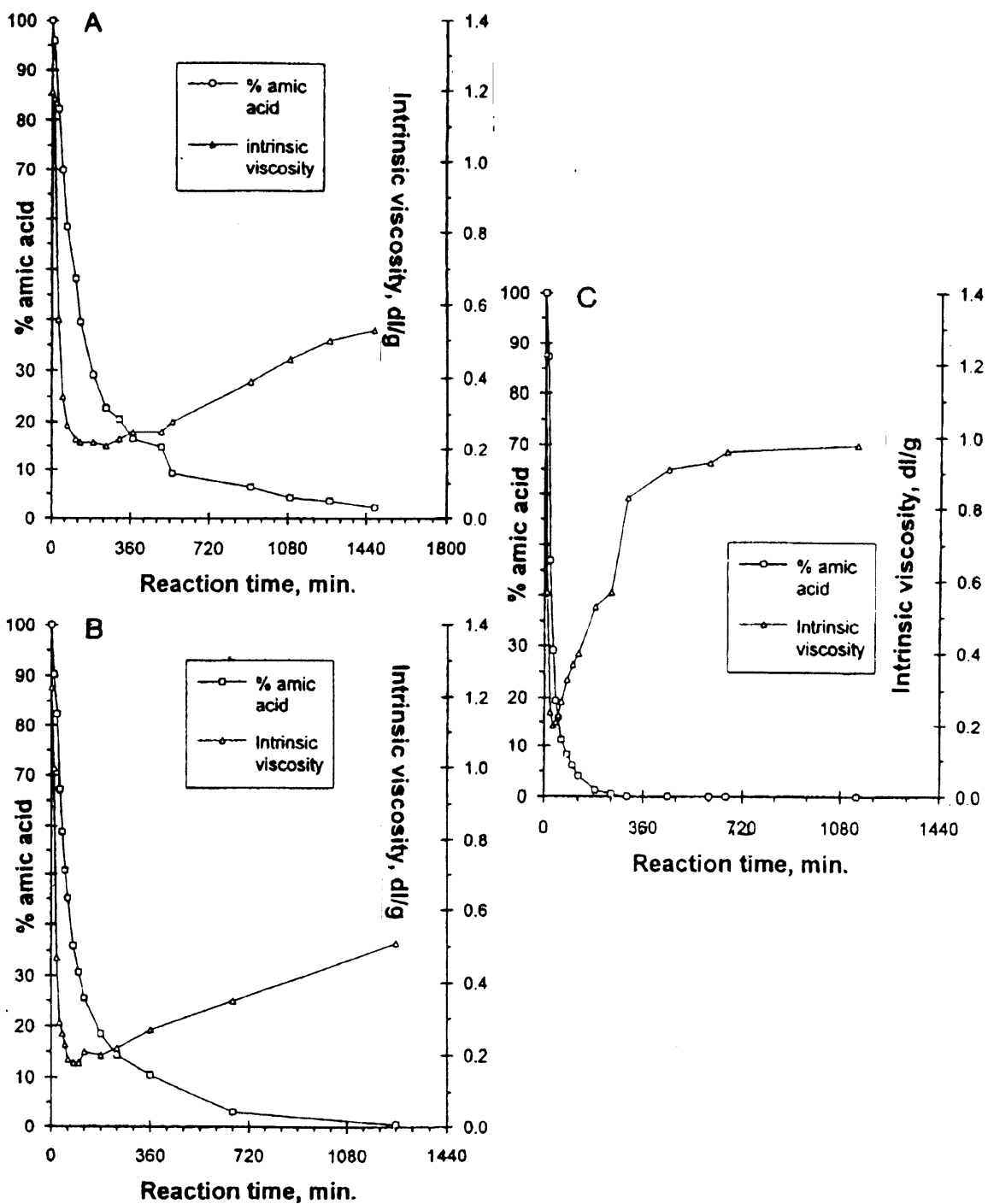


Figure 2.2.1.3.1 Remaining Amic Acid Content and Intrinsic Viscosity as a Function of Reaction Time: (A) at 140°C; (B) at 150°C; (C) at 180°C<sup>21</sup>

hydrolyzed due to the ortho-carboxyl group which promotes nucleophilic attack of water, leading to chain scission.<sup>1</sup>

#### **2.2.1.4 Chemical Imidization**

Cyclodehydration of PAAs can be accomplished at room temperature or slightly higher with chemical reagents (Scheme 2.2.1.4.1).<sup>19,26,27</sup> Various combinations of chemical reagents have been used to affect this conversion. The preferred product of the reaction, either a polyimide (III-a) or a polyisoimide (III-b), will be determined by the selection of chemical reagent. Dehydrating agents such as anhydrides of carbonic, formic and acetic acids can be used in conjunction with a tertiary amine such as pyridine, 2-methylpyridine, triethylamine, and isoquinoline, to bring about the polyimide formation. The mechanism of formation involves a mixed anhydride intermediate followed by an iminolactone and then the imide linkage, which is the thermodynamically favored product (Scheme 2.2.1.4.1-III-a).<sup>28</sup>

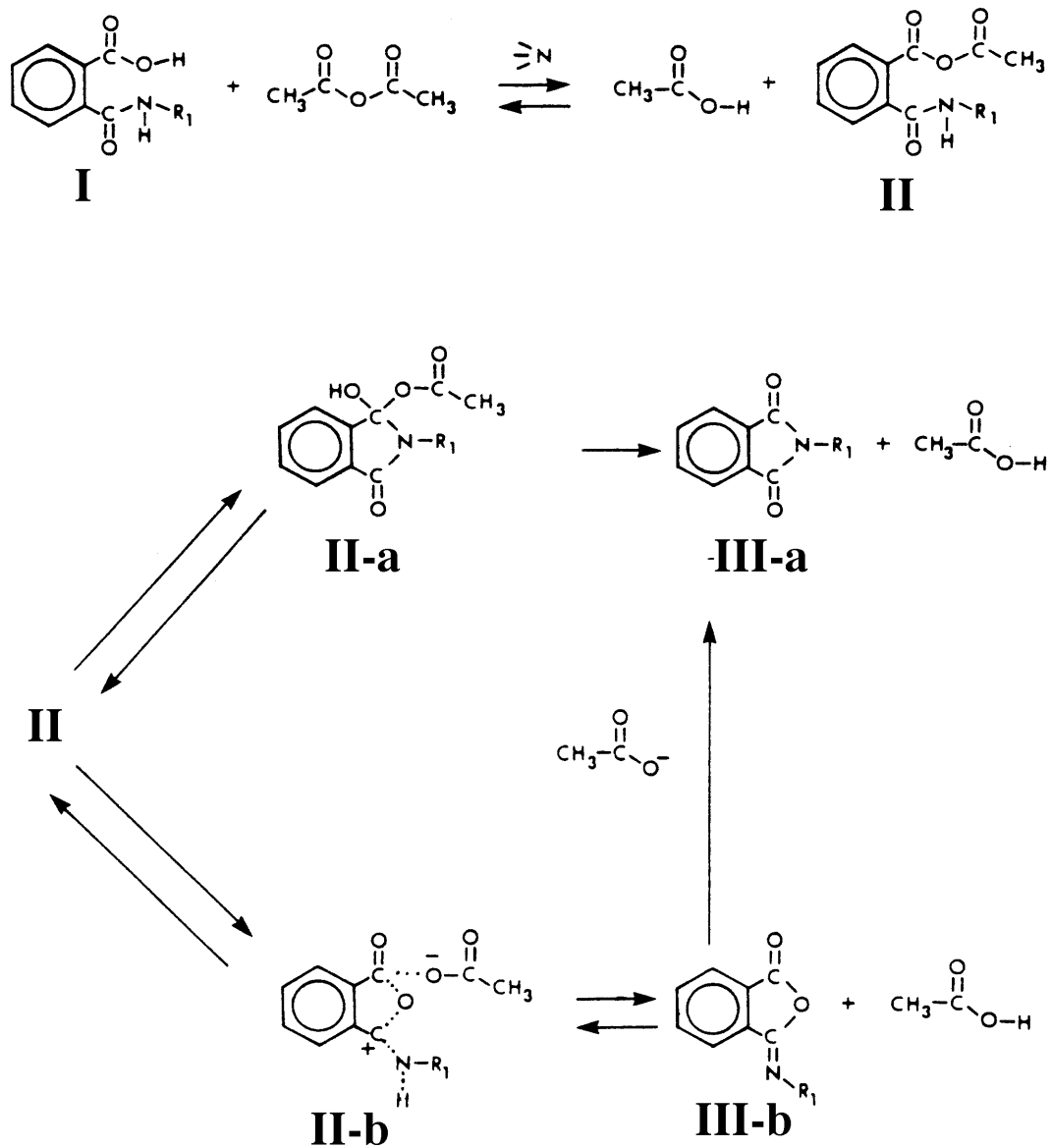
Alternatively, PAAs can also be converted to the polyisoimide with a number of other chemical reagents (Scheme 2.2.1.4.1-III-b).<sup>29-32</sup> A combination of pyridine and trifluoroacetic anhydride favor isoimide formation.<sup>31</sup> The polyisoimides can be thermally converted to the polyimide or they can serve as reactive intermediates.<sup>33</sup> Post-reactions of polyisoimides with amines, alcohols, thiols or hydrazoic acid result in poly(amide-imide), poly(amide-ester), poly(amide-thioester) and polytetrazole acid, respectively.

Landis prepared a number of polyisoimide oligomers with thermally curable endgroups.<sup>34,35</sup> He found that polyisoimides are more soluble than their related polyimide structure. In fact, the most significant feature of polyisoimides is improved solubility/processability over that of polyimides.

### **2.2.2 Additional Routes to Polyimides**

#### **2.2.2.1 Polyimides From Dianhydrides and Diisocyanates**





Scheme 2.2.1.4.1 Chemical Imidization and Isoimidization of Poly(amic acid)s<sup>32</sup>

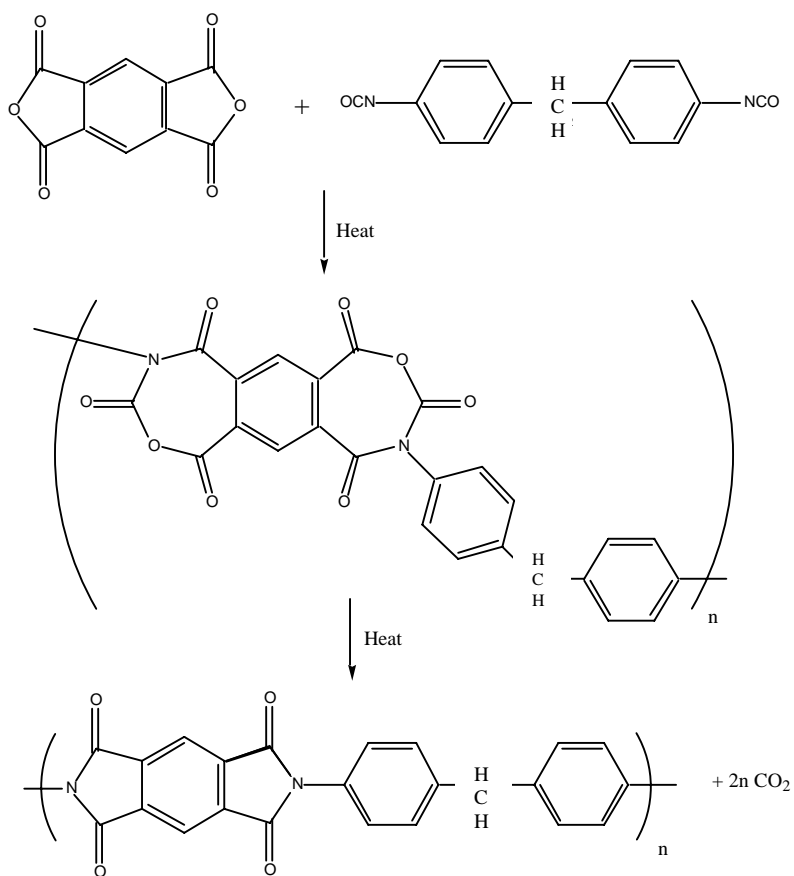
Dianhydrides and diisocyanates can react to form polyimides with elimination of carbon dioxide as a byproduct. Although the mechanism has not been fully elucidated, it has been proposed that it proceeds through an imide-anhydride seven-membered ring at 40°C (Scheme 2.2.2.1.1).<sup>36</sup> Upon further heating, carbon dioxide is liberated and the polyimide is formed. Many of the earlier polymers prepared using this route were found to have low molecular weight and to be insoluble. More recently, the catalyst induced formation of polyimides in dipolar solvents using alkali metal alkoxides and phenoxide yielded high molecular weight polymers.<sup>37,38</sup> Kakimoto et al. has recently reported obtaining soluble polyimides in benzonitrile using bulky diisocyanates (Scheme 2.2.2.1.2).<sup>39</sup>

The potential for side reactions is one of the drawbacks in using this preparation method. For example, isocyanates can undergo dimerization, cyclotrimerization, and even polymerization to form nylon-1.<sup>40</sup>

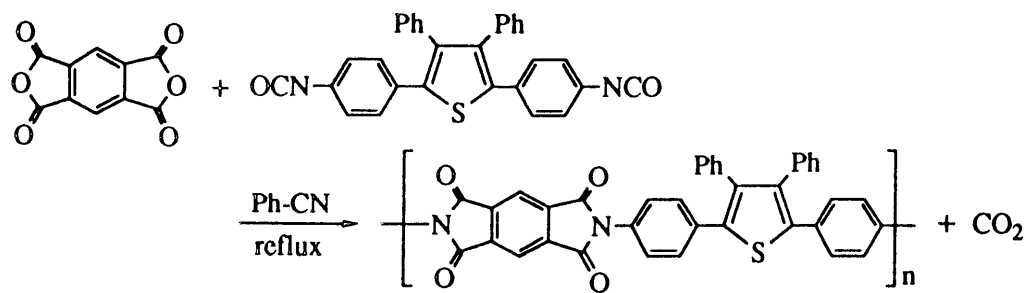
#### ***2.2.2.2 Nucleophilic Aromatic Substitution***

Nucleophilic aromatic substitution reactions are well known synthetic methods for preparing poly(arylene ether-ketone)s and poly(arylene ethersulfone)s and may be used to form ether or sulfide linked polyimides (commercially available Ultem could be produced using this route).<sup>41</sup> To form the polyimides, a strongly activated bis-aromatic halo-<sup>42,43</sup> or nitro-<sup>44-46</sup> monomer containing precyclized imide moieties was reacted in a dipolar aprotic solvent with either a bisphenol or bithiol salt (Scheme 2.2.2.2.1).<sup>47</sup> The intermediate encountered, enroute to the final product, is the Meisenheimer complex, which is effectively stabilized through resonance by the imide system (Scheme 2.2.2.2.2).<sup>48</sup>

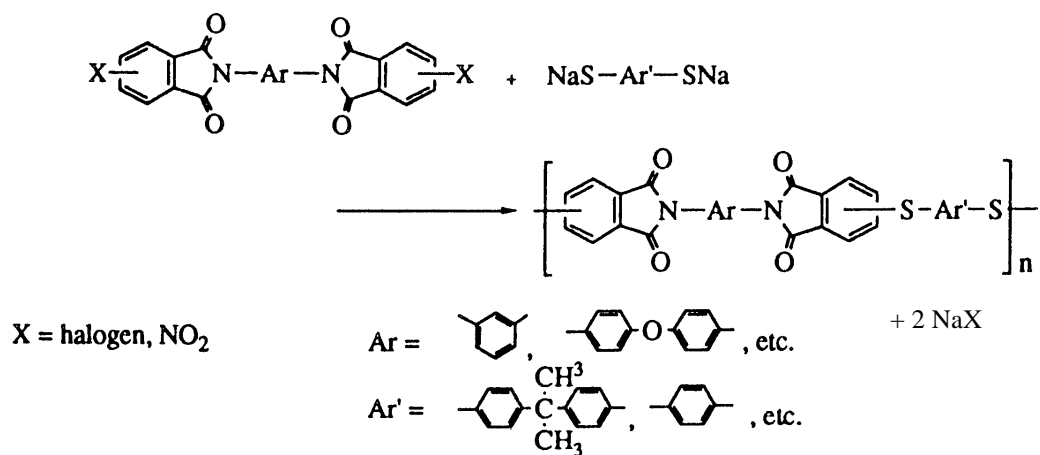
Recently, Kricheldorf et al.<sup>49,50</sup> modified this procedure for polyarylene ethers to bypass the use of oxygen-sensitive anhydrous bisphenol salts and to eliminate the need for removal of the salt by-product from the reaction (Scheme 2.2.2.2.3). Others have employed this methodology using an A-B type monomer to form polyimides (Figure 2.2.2.2.1).<sup>51</sup>



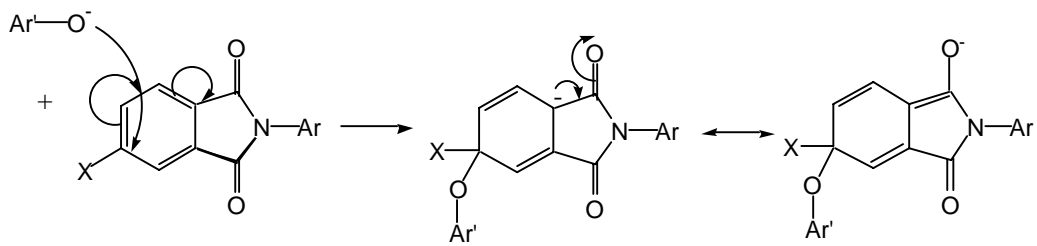
Scheme 2.2.2.1.1 Proposed Route to Polyimides from Dianhydrides and Diisocyanates via an Imide-Anhydride Seven-Membered Ring<sup>36</sup>



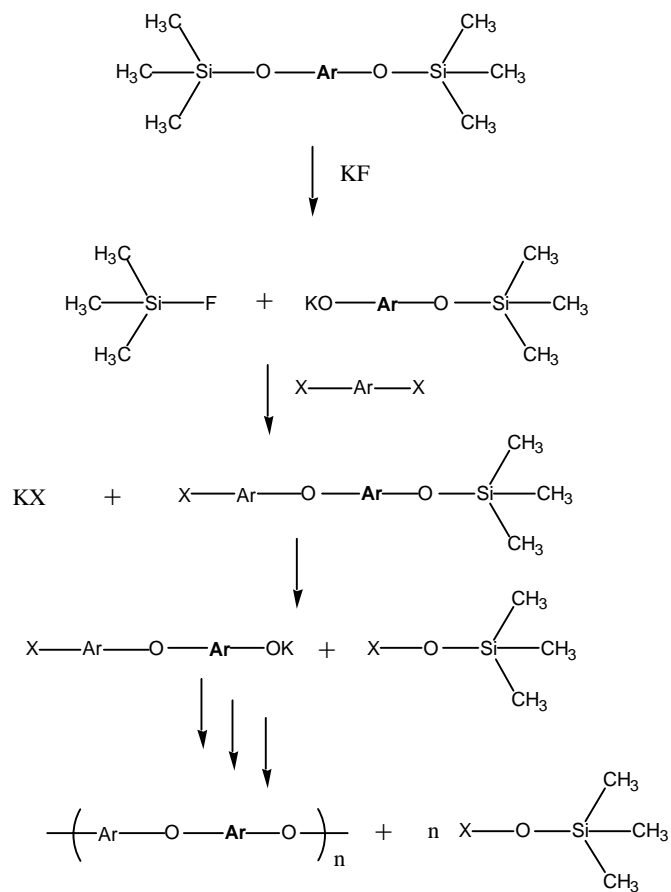
Scheme 2.2.2.1.2 Preparation of a Polyimide from a Dianhydride and a Diisocyanate with Bulky Substituents<sup>39</sup>



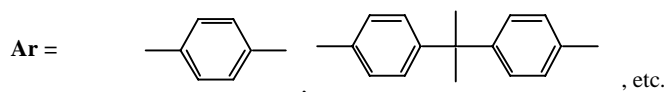
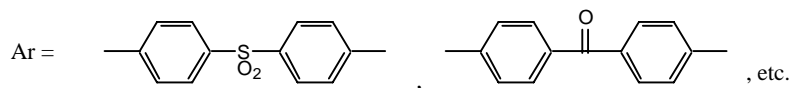
Scheme 2.2.2.2.1 Synthesis of Polythioetherimides by Aromatic Nucleophilic Substitution<sup>47</sup>



Scheme 2.2.2.2.2 The Meisenheimer Transition State<sup>48</sup>



X = F, Cl, Br, etc.;



Scheme 2.2.2.2.3 Synthesis of Polyarylene Ethers from Bis(trialkylsilyl)ethers of Bisphenols and Activated Bishalo Compounds<sup>49,50</sup>

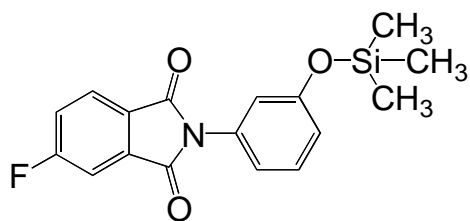


Figure 2.2.2.2.1 A-B Type Monomer to Form Polyimides<sup>51</sup>

### 2.2.2.3 Ester-Acid Route

The ester-acid precursor method for polyimides can be employed with aromatic diamines in solution.<sup>52</sup> In this synthetic route, the monomeric dianhydride is pre-reacted with an alcohol such as methanol or ethanol to form the o-ester-acid of the dianhydride (Scheme 2.2.2.3.1).<sup>52</sup> This reaction can be catalyzed by a tertiary amine such as triethylamine. Huang et al. recently reported on the ring opening selectivity of various dianhydrides toward alcohols (Figure 2.2.2.3.1).<sup>53</sup> The isomeric ratios of diester-diacids were found to be independent of alcohol structure but quantitatively correlated with the electron affinities of the different bridging groups (Scheme 2.2.2.3.2 & Table 2.2.2.3.1).<sup>53</sup>

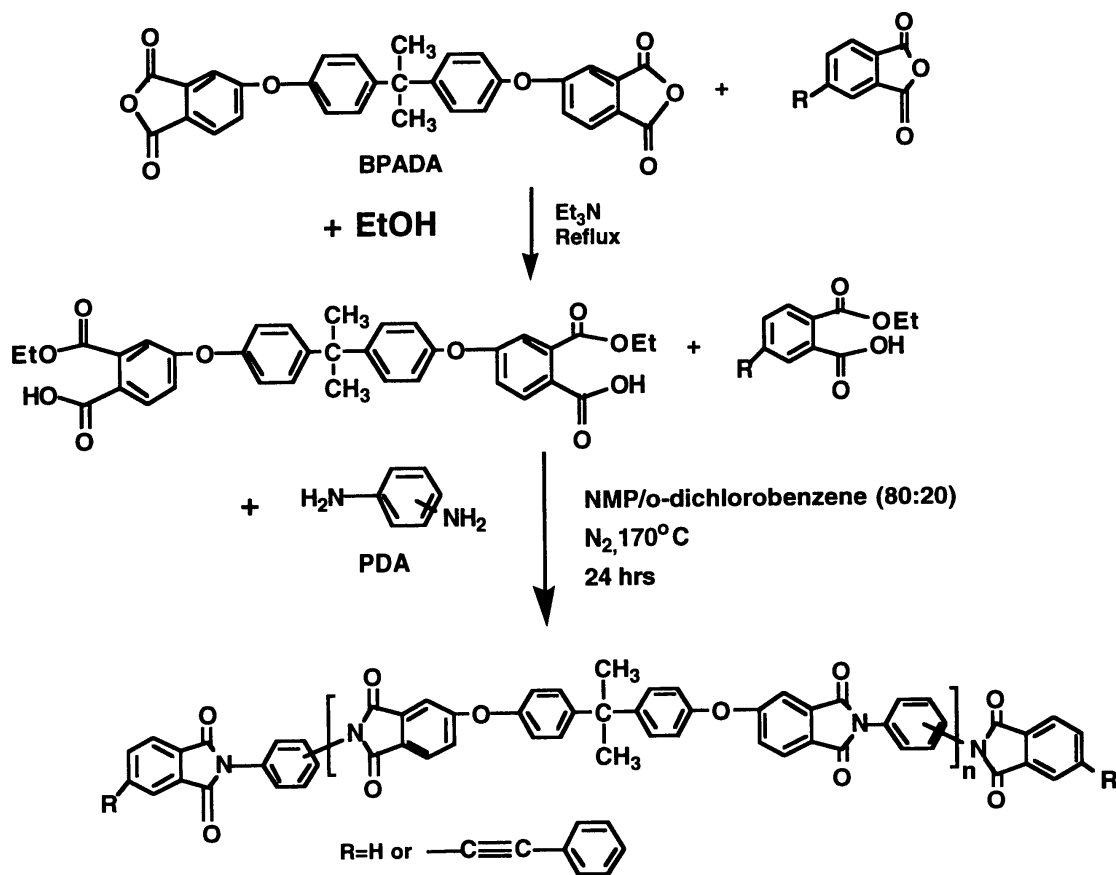
The resulting isomeric diester-diacids are much more soluble and are possibly less toxic than the corresponding dianhydrides. Additionally, they are relatively stable towards moisture. Essentially, the ester-acid acts as a protecting group for the otherwise hydrolytically unstable anhydride. A commercial example typically synthesized by the ester-acid route is the thermosetting PMR-15 resin (Polymers from Monomeric Reagents,  $M_n \sim 1,500$ g/mole) (Scheme 2.2.2.3.3).<sup>54</sup>

It has been shown that at higher temperatures (100-150°C) the anhydride functionality is reformed from the ester-acid.<sup>55</sup> The work of Moy et al. proved that nucleophilic attack on the ester carbonyl by the diamine did not occur.<sup>55</sup> Instead the ester-acid reverts to the anhydride at elevated temperatures (eg. >140°C) thereby becoming reactive toward amines. Consequently, the rapid formation of amic acid ensues, followed by cyclodehydration to form polyimide at these high temperatures. This process has the advantage of being a 'one-pot' reaction.<sup>56</sup>

### 2.2.2.4 Transimidization

High molecular weight homo- or co-polyimides can also be prepared via a transimidization reaction involving an amine-imide exchange with either aromatic or aliphatic diamines, or aminopropyl functional siloxane oligomers (Scheme 2.2.2.4.1).<sup>57-60</sup> The driving force for the bis(etherimide)-diamine exchange is the production of a less





Scheme 2.2.2.3.1 Synthesis of Phthalic Anhydride and/or Phenylethynyl Phthalic Anhydride Endcapped Polyimides via the Ester-Acid Route<sup>52</sup>

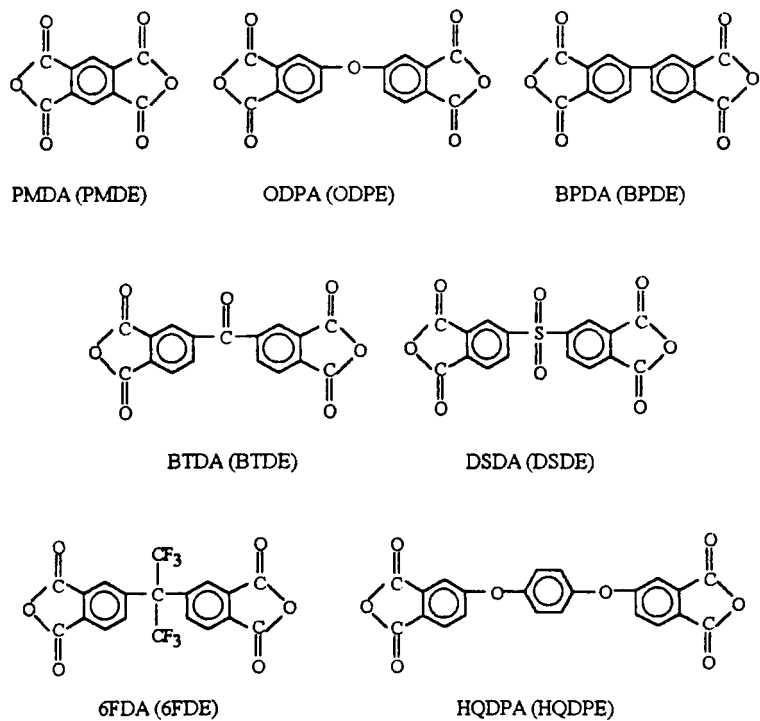
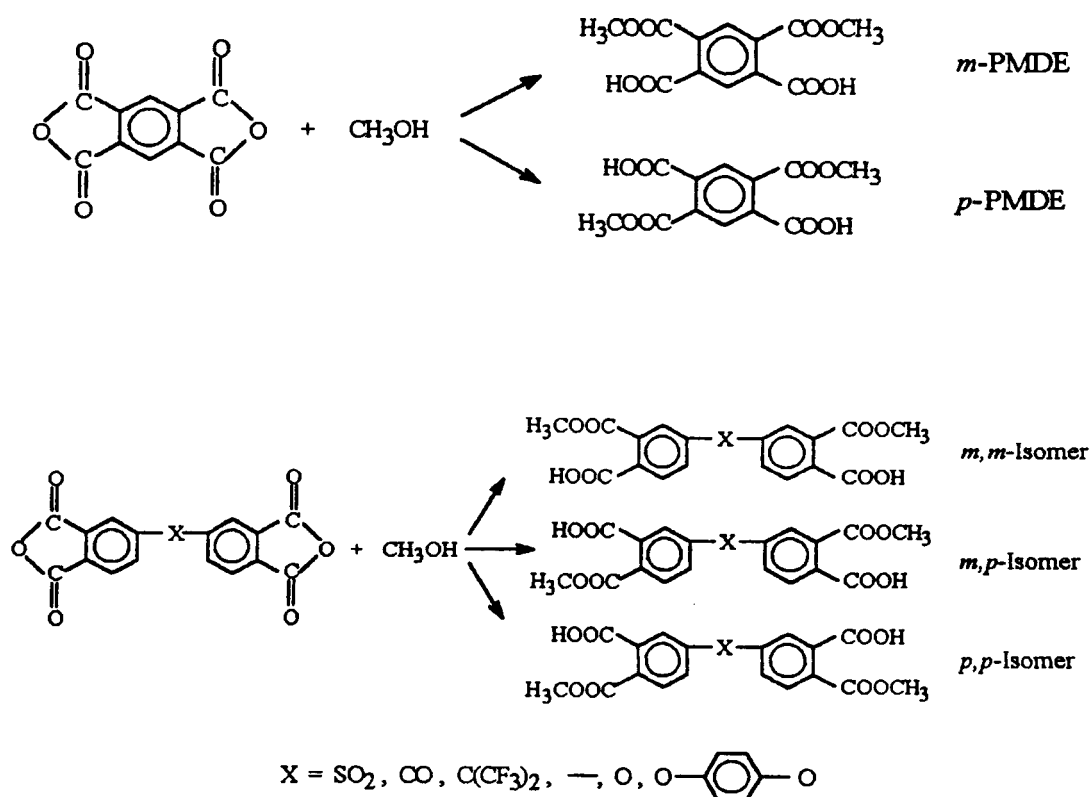


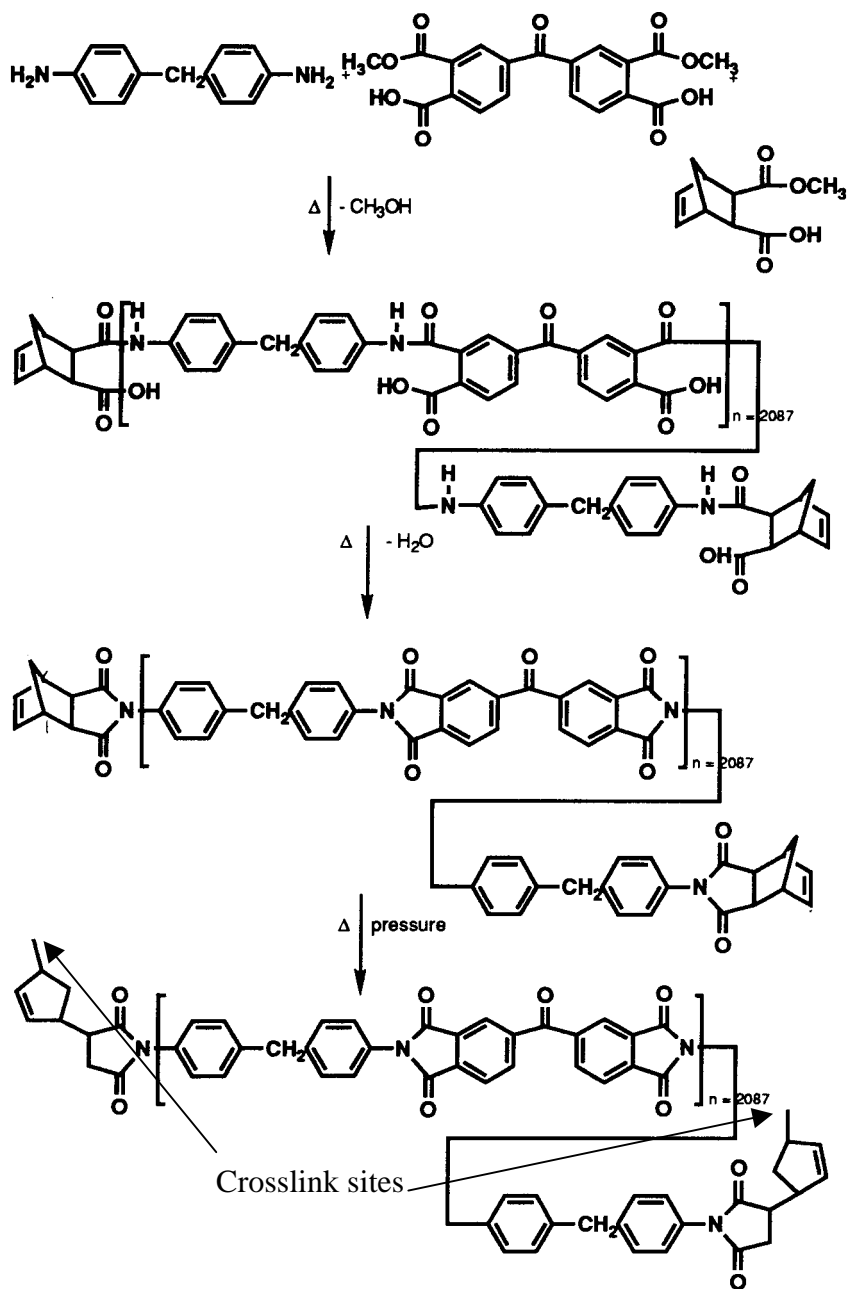
Figure 2.2.2.3.1 Dianhydrides for Methanolysis Reactions<sup>53</sup>



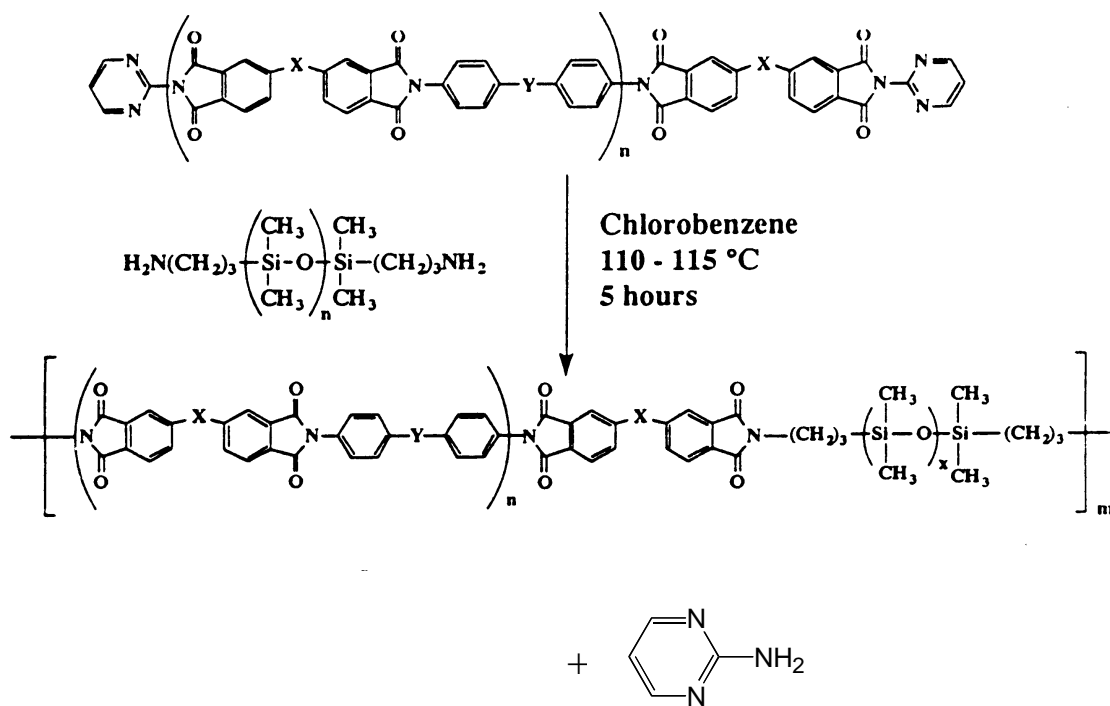
Scheme 2.2.2.3.2 Synthesis of the Three Isomers of Diester-Diacids Prepared from Bridged Dianhydrides<sup>53</sup>

Diester-diacids	EA <sup>+</sup>	Relative abundance	
		<i>Para</i>	<i>Meta</i>
DSDE	1.57	0.62	0.38
BTDE	1.55	0.57	0.43
6FDE	—	0.52	0.48
BPDE	1.38	0.43	0.57
ODPE	1.30	0.34	0.66
HQDPE	1.19	0.26	0.74

Table 2.2.2.3.1 E<sub>a</sub> (eV) and Relative Abundance of *meta*- and *para*-positions<sup>53</sup>



Scheme 2.2.2.3.3 PMR-15 Resin Chemistry Utilizing the Ester-Acid Route<sup>54</sup>



Scheme 2.2.2.4.1 Synthesis of Perfectly Alternating Segmented Imide Siloxane Copolymers<sup>60</sup>

basic byproduct. To obtain high molecular weight polymer, the difference in basicities must be large or the diamine byproduct must be removed during the reaction. It has been found that even though the reaction equilibrium favors the starting material when a more basic amine is the byproduct, a number of catalysts, such as carboxylate salts of zinc, lead, and cadmium, can be used to form high molecular weight polyimides.<sup>61</sup> Webb et al.<sup>62</sup> and Takekoshi et al.<sup>58</sup> demonstrated that 2-amino pyridine is readily exchanged by common aromatic diamines.

#### ***2.2.2.5 Other Routes to Polyimide Formation***

Many other polyimide preparation methods have been reported in addition to the aforementioned routes. Due to the improved stability and solubility of derivatized PAAs, a number of techniques have been developed to form alkyl esters,<sup>63-67</sup> silyl esters,<sup>68,69</sup> and ammonium salts<sup>70,71</sup> of PAAs, all of which can be thermally cyclized to form polyimides. The alkyl esters are formed from the reaction of an ester-acid chloride and the silylated esters are formed in the reaction of N,N'-bis(trialkylsilyl) diamines with various dianhydrides. The ammonium salts of PAA's can be formed by reaction with a secondary or tertiary amine. The resulting polyelectrolyte can then be dispersed in an aqueous medium and used to fabricate carbon fiber composites.<sup>71</sup>

Polyimides can also be prepared by Diels-Alder<sup>72-75</sup> and Michael<sup>76,77</sup> cycloaddition reactions. Palladium catalyzed carbon-carbon coupling reactions have also been reported in the literature<sup>78,79</sup> as well as methods utilizing a 'one-step' process which bypasses the PAA precursor.<sup>80,81</sup>

## 2.3 Polyimide Properties and Applications

### 2.3.1 Characterization and Properties of Polyimides

#### 2.3.1.1 *Molecular Weight and Functional Group Analysis via Titration Measurements*

Precise control of molecular weight, molecular weight distribution, and reactive groups is an important goal of polymer science. Left undetermined these parameters can significantly effect polymer properties. For example, while polymers may have identical repeat units and number average molecular weights, their polydispersities may be different. Polymers with different polydispersities can greatly influence thermal and mechanical properties.<sup>82,83</sup> In addition, specific functional groups are known to influence polymer crystallization<sup>84</sup> and lead to crosslinking side reactions.<sup>85</sup> In order to probe these important polymer parameters, exact techniques for measuring these parameters are needed.

Molecular weight determination is of primary importance in polymer science due to the number of inherent properties this parameter reflects. Solubility is required for determining polymer molecular weight by solution techniques. Unfortunately, many polyimides are insoluble due to crystallinity, chain rigidity or network formation. Although many polyimides are insoluble, their precursor polyamic acids (PAAs) are soluble. However, hydrolytic instability of the o-carboxylic amide linkage requires that careful procedures need to be followed to correctly assess molecular weight. Soluble polyimides can be fully characterized more easily.

Solution viscosity is perhaps the easiest method to investigate viscosity average molecular weight. It is a very useful technique, especially if the empirical Mark-Houwink constants have been determined. However, the molecular weight distribution cannot be assessed and it is necessary to utilize additional techniques to better define the system.

The technique most widely used for investigating molecular weight is gel permeation chromatography (GPC), which is also known as size exclusion chromatography (SEC). When properly calibrated, GPC allows the determination of the number-, viscosity-, weight- and 'z'- average molecular weights. Moreover, the polymer-

solvent pair constants,  $K$  and  $a$ , and the radius of gyration,  $R_g$ , can also be determined. Grubisic et al.<sup>86</sup> showed that polymers with the same hydrodynamic volume elute from a column at the same volume, regardless of chemical nature and architecture. The product of intrinsic viscosity and molecular weight is used to define this parameter, which has been termed Universal Calibration.

It is common to use a series of nearly monodisperse polystyrene samples of varying molar mass to generate a calibration curve for GPC. Thus, it is common to report molecular weights relative to those of polystyrene standards. However, in many cases the actual molecular weight value can be quite different. This problem can be eliminated if the GPC is coupled to a viscosity detector allowing the absolute molecular weight to be determined via the universal calibration procedure.

Konas et al.<sup>87,88</sup> found that good mobile phases for polyimides were among the following: chloroform, tetrahydrofuran, N-methylpyrrolidone (NMP) with 0.06M LiBr, or NMP stirred over  $P_2O_5$  before use. The addition of lithium bromide and  $P_2O_5$  eliminated spurious high molecular weight peaks, which suggests that they suppress specific polyelectrolyte or other similar effects.<sup>87</sup>

Functional group analysis via titration experiments is a complimentary technique to GPC. Titration experiments may be conducted to determine the concentration of a particular reactive group in the polymer. It can also reveal the extent of imidization by determining the percent residual carboxylic acid groups. Titration also enables measurement of the number average molecular weight of polymers based on reactive endgroups. To establish a well-defined polyimide system, endgroup titration results, as well as spectroscopic endgroup analysis, can be correlated with the molecular weight data obtained from GPC.

Other important techniques used to determine polymer molecular weight include membrane osmometry (for  $M_n$ ),<sup>89</sup> light scattering (for  $M_w$ ),<sup>89,90</sup> and low angle laser light scattering (LALLS) (for  $M_w$ ).<sup>91,92</sup>

### 2.3.1.2 *Structural Characterization*



A number of structural changes occur during polyamic acid formation and subsequent imidization. Several methods, including Fourier transform infrared (FTIR), Raman and UV spectroscopies, as well as  $^1\text{H}$ ,  $^{13}\text{C}$ ,  $^{15}\text{N}$  and  $^{19}\text{F}$  NMR spectroscopies have been used to understand these chemical transformations.<sup>96</sup>

Functional groups are conveniently measured using FTIR. Characteristic absorptions are observed for the imide, anhydride, amine, isoimide and amic acid moieties. Table 2.3.1.2.1 lists the absorption bands for each of these structures.<sup>93-95</sup> Although a great deal of structural information can be found in the later stages of imidization, FTIR cannot detect small amounts of uncyclized amic acid groups due to low sensitivity. However, FTIR can give semiquantitative data on the imidization process.<sup>96</sup>

NMR spectroscopy may also be used to monitor the imidization process. Imide conversion can be monitored from the  $^1\text{H}$  NMR signal intensities of COOH protons. In one system, imidization was initiated at 70°C and was completed at 200°C.<sup>97</sup>  $^{13}\text{C}$  NMR spectroscopy has been utilized to monitor thermal and chemical imidization as well as depolymerization.<sup>98</sup>  $^{19}\text{F}$  NMR has also been conducted on fluorine-containing polyimides and the results were found to correlate with carbon-fluorine coupling constants.<sup>99</sup>

### 2.3.1.3 *Glass Transition Temperature and Thermal Stability*

The glass transition temperature ( $T_g$ ) is the temperature at which a polymer undergoes extensive cooperative segmental motion along the backbone. The  $T_g$  may also be described as the relaxation point which occurs between the glassy and rubbery plateaus. A number of intra- and intermolecular interactions may affect the  $T_g$ , including electrostatic and ionic interactions, hydrogen bonding, chain packing efficiency and chain stiffness. In particular, the chain stiffness has been found to affect the  $T_g$  to a great extent.

Differential scanning calorimetry (DSC), among other analytical methods, is routinely utilized to probe the  $T_g$  of polymers by monitoring the heat capacity as a function of temperature. The  $T_g$  is a second order endothermic transition.

Table 2.3.1.2.1 Infrared Absorption Bands of Imides and Related Compounds<sup>93-95</sup>

	<b>Absorption band</b>		
	<b>(cm<sup>-1</sup>)</b>	<b>Intensity</b>	<b>Origin</b>
<b>Aromatic imides</b>	1780	s	C=O asym. Stretch
	1720	vs	C=O sym. Stretch
	1380	s	C-N stretch
	725		C=O bending
<b>Isoimides</b>	1795-1820	s	Iminolactone
	1700	m	Iminolactone
	921-934	vs	Iminolactone
<b>Amic acids</b>	2900-3200	m	COOH and NH(2)
	1710	s	C=O (COOH)
	1660 amide I	s	C=O (CONH)
	1550 amide II	m	C-NH
<b>Anhydrides</b>	1820	m	C=O
	1780	s	C=O
	720	s	C=O
<b>Amines</b>	3200 two bands	w	NH(2) sym. Structure (v(s)) NH(2) asym. Structure (v(as)) $v(s) = 345.53 + 0.876*v(as)$

vs, very strong; s, strong; m, medium; w, weak

Table 2.3.1.3.1 shows the  $T_g$ s of four BTDA based polymers that differ in diamine structure.<sup>102</sup> The  $T_g$  increases with chain stiffness which is a function of the diamine bridging unit in the BTDA series. The methylene-bridged diamine allows a greater degree of bond rotation about the linking group, leading to the lowest  $T_g$ . Similarly, the flexible ether-linked diamine lowers  $T_g$ . However, by changing the bridging group to a carbonyl, the  $T_g$  increases, due to an increase in chain rigidity. Chain rigidity is a function of the reduced rotation about the  $-(O)C$ -aryl single bond, which has more double bond-like character. The sulfone linkage has strong electron withdrawing capabilities, which causes the  $T_g$  to continue increasing, even though the out-of-plane, bulky  $SO_2$  functionality could potentially hinder chain packing. Again, the higher  $T_g$  for this system could be related to more double bond like character between the bridging and aryl groups.

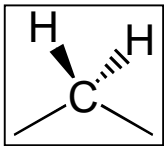
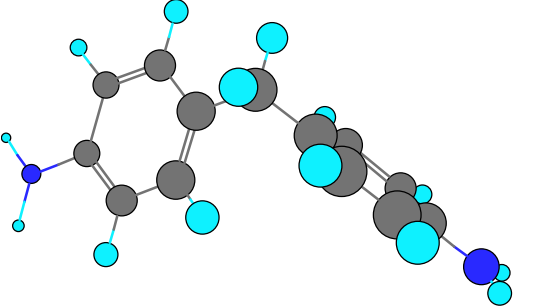
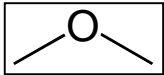
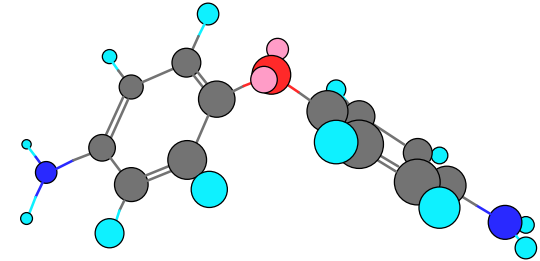
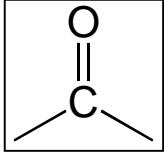
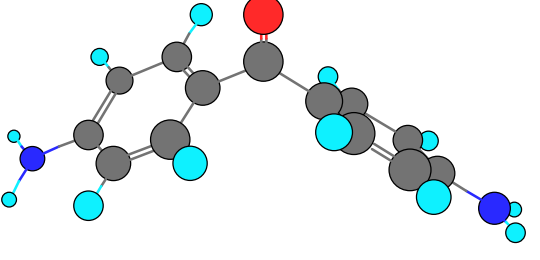
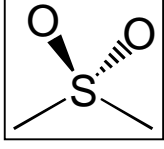
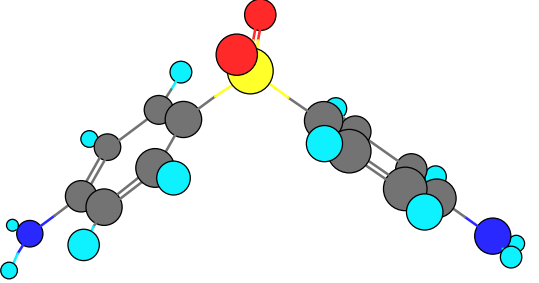
Bell et al.<sup>103</sup> has reported the influence of diamine catenation on  $T_g$ . From Table 2.3.1.3.2, it is clearly illustrated that *ortho* and *para* linked systems lead to higher  $T_g$ s when compared to their *meta* linked counterparts. The presence of *ortho* and *para* linked benzophenone diamine moieties can give rise to a strong dipolar unit,<sup>103</sup> thereby decreasing chain flexibility.

The thermal stability of polymers is often analyzed by thermogravimetric analysis (TGA) either under air or nitrogen. TGA monitors polymer weight loss as a function of temperature either under dynamic or isothermal conditions. Under dynamic conditions (10°C/min) the 5% weight loss value is often over 500°C for wholly aromatic polyimides. Chemical moieties that decrease the thermal stability of polyimides may be aliphatic or benzylic protons; hydroxyl groups and other less thermally stable functionalities.

#### 2.3.1.4 *Insolubility/Infusibility*

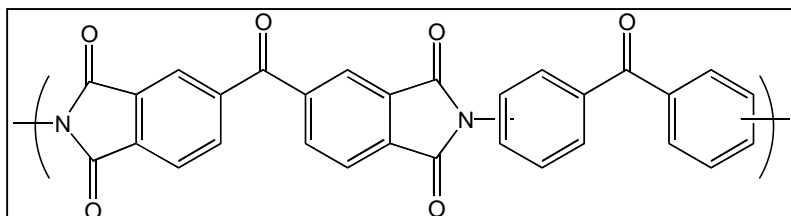
Insolubility and infusibility of some polyimides has been attributed to crosslinks formed during the imidization process. Although this is undoubtedly true in some cases, there are other possible causes such as charge transfer complexes<sup>100</sup> and semi-crystallinity.<sup>101</sup> For the PMDA/ODA polyimides, crosslinking cannot be the sole

Table 2.3.1.3.1 The Effect of Bridging Unit on the Glass Transition Temperature ( $T_g$ )<sup>102</sup>

Diamine Bridge (X)	Diamine 3-D Rendering	$T_g$
		234*
		236
		255
		273

\*Cured to 300 deg. C in vacuum

Table 2.3.1.3.2 The Effect of Catenation on the Glass Transition Temperature ( $T_g$ )<sup>103</sup>



<b>Diamine Catenation</b>	<b><math>T_g</math> (°C)</b>
2,2'	285
3,3'	232
4,4'	290

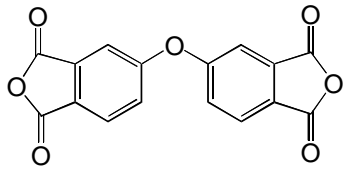
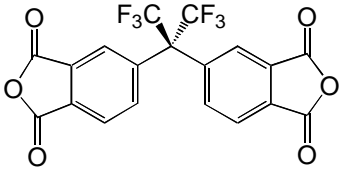
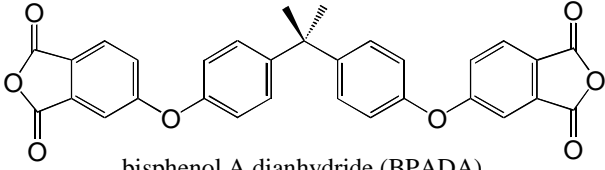
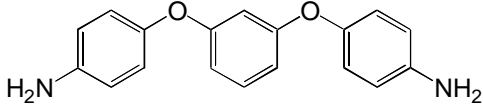
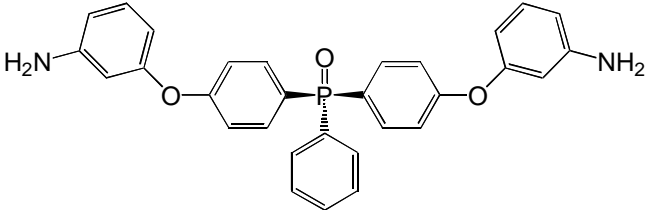
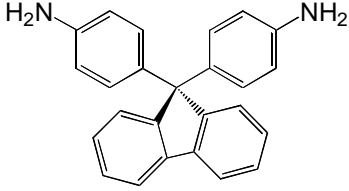
contributor to insolubility because although these systems are insoluble in common organic solvents, they are fully soluble in concentrated sulfuric acid.

Often, insolubility is due to very rigid macromolecular chains. Improvement in polymer solubility has been accomplished in at least four ways.<sup>102</sup>

1. Polar groups have been placed either pendant to or along the backbone
2. Bulky groups have been employed as either pendant or bridging groups
3. Chain flexibility has been promoted by *ortho* and *meta* catenation versus *para* catenation
4. Chain flexibility has been promoted by linking groups with greater rotational freedom, such as, -O-, -CH<sub>2</sub>-, -SO<sub>2</sub>-, -(CH<sub>3</sub>)<sub>2</sub>- and -C(CF<sub>3</sub>)<sub>2</sub>-.

Table 2.3.1.4.1 presents some monomers that may increase solubility when incorporated into polyimides based on their chemical structural features.

Table 2.3.1.4.1 Common Dianhydrides and Diamines with Various Structural Features

Dianhydride/Diamine	Category
	1,4
4,4'-oxydiphthalic anhydride (ODPA)	
	2,4
hexafluoroisopropylidene dianhydride (6FDA)	
	1,4
bisphenol A dianhydride (BPADA)	
	1,3,4
1,3-bis(4-aminophenoxy)benzene (TPER)	
	1,2,3,4
bis-(3-aminophenoxy-4'-phenyl) Phenylphosphine Oxide (m-BAPPO)	
	2
9,9-bis(4-aminophenyl) Fluorene (FDA)	

## 2.3.2 Polyimide Applications

### 2.3.2.1 Polyimides in Electronics

Polymers are widely used in the electronics field in areas such as wafer fabrication, adhesion, chip packaging and assembly.<sup>104-111</sup> Polyimides have found a great deal of utility in wafer fabrication as photoresists due to their excellent performance at elevated temperatures, corrosion resistance and their ability to be spin-coated onto substrates. They also serve as insulators, which prevent “cross-talk” between conducting vias, and as adhesives between polymer-polymer and polymer-metal interfaces. Polyimides may also be designed so that their coefficient of thermal expansion (CTE) more closely matches that of the supporting substrate, which is generally a metal (Figure 2.3.2.1.1).<sup>112</sup> By matching the CTE of the metal, the polyimide-metal interface experiences very little stress associated with thermal cycling, which otherwise may cause premature failure.

Photosensitive polyimides are used in electrical devices where a submicron pattern is needed to route electrical current. They also eliminated the complex multistep processing used in the high-resolution photolithography process needed for nonphotosensitive materials. The properties of a photosensitive polyimide are changed upon exposure to light. The exposed portion of the polyimide undergoes crosslinking or scission chemical changes that either inhibit or promote solubility, respectively. If light exposure inhibits solubility, the polymer is said to be negatively-imaged.<sup>113,114</sup> However, if light exposure promotes solubility the resin is said to respond positively.<sup>115</sup>

A typical negative-imaging photosensitive polyimide is shown in Figure 2.3.2.1.2.<sup>115</sup> Upon exposure to light, the derivatized polyamic acid undergoes crosslinking which renders it insoluble. The unexposed region, which is still relatively soluble, can be removed by solvent development. The final curing step causes the cleavage and volatilization of the crosslink while simultaneously forming the heterocyclic imide structure. A negative-image response can also be promoted through polyimide in-chain functionalities which are photo-excitabile. The most widely known polyimide of this



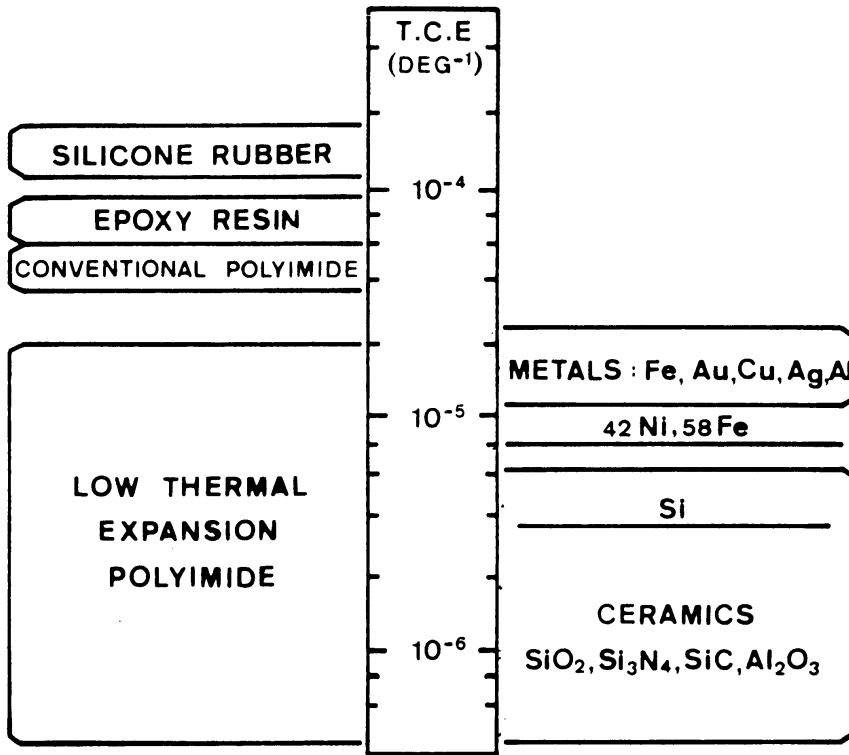


Figure 2.3.2.1.1 The Coefficient of Thermal Expansion of Various Metals, Ceramics and Organic Polymers<sup>112</sup>

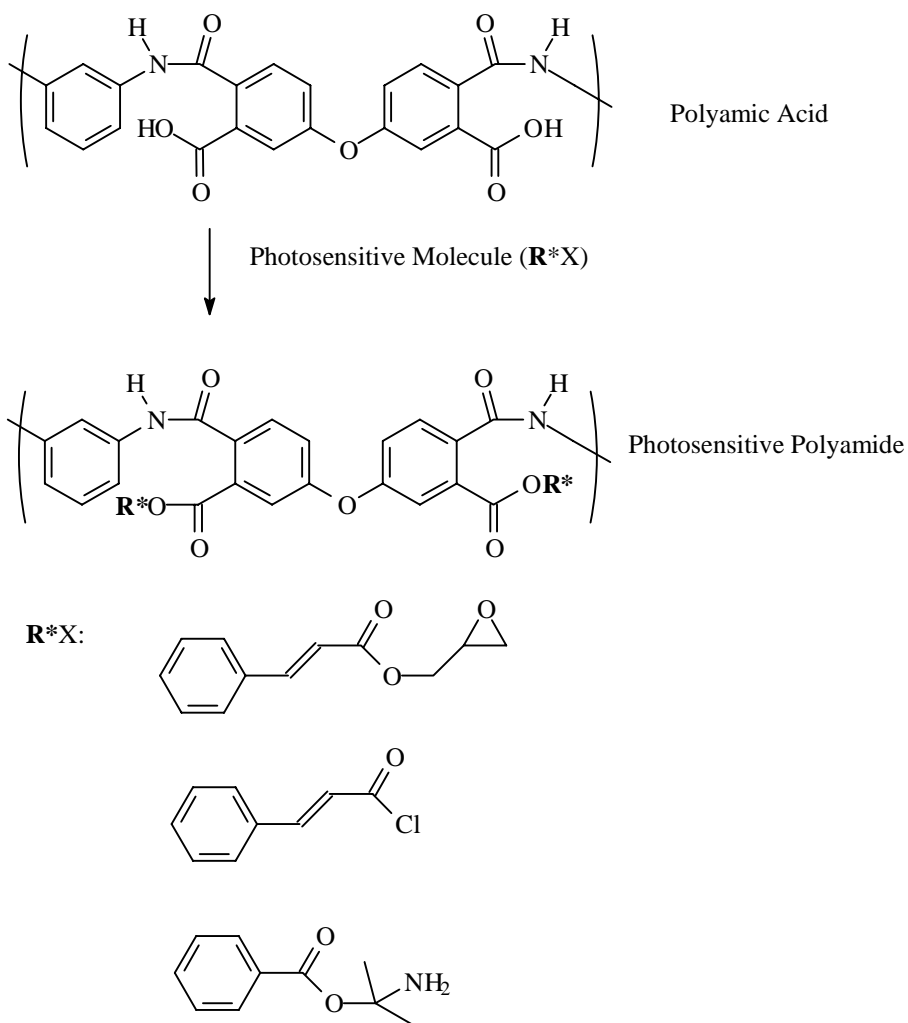


Figure 2.3.2.1.2 Typical Negative-Imaging Photosensitive Polyimide<sup>115</sup>

type contains a photosensitive benzophenone carbonyl and labile benzylic or methylene protons, which can be abstracted by the excited carbonyl moiety. An interchain bond is formed when two carbon radicals combine to form a carbon-carbon bond. These materials have the advantage of being fully cyclized before exposure, which allows the shrinkage upon curing to be greatly reduced.

Positive photoresist polyimides<sup>116-119</sup> become more soluble when exposed to the correct wavelength of light. An increase in solubility is observed when the backbone undergoes cleavage or when the polarity of side groups changes. Ho et al.<sup>117</sup> recently reported silylating hydroxyl groups in a polyimide backbone. The trimethoxysilane bond was found to undergo hydrolysis in the presence of a photoacid-generating molecule. The solubility differential between the silylated and non-silylated polyimide allowed them to be selectively developed.

#### 2.3.2.2 *Polyimides as Optical Waveguides*

The function of an optoelectronic device is to convert electrical signals to optical signals, transport the signals through space, and reconvert them to electrical signals. Optical waveguides are reflective channels which allow information in the form of light to be transported through a medium by internal reflection.<sup>120</sup> Optical waveguides have the advantage of being able to transport multiple signals simultaneously without affecting each other while having both immunity to electromagnetic interference, and noninteraction when signals cross.<sup>121</sup> The prevailing method for telecommunication relies heavily on optoelectronic devices.

Both freestanding and embedded waveguides are well known.<sup>121</sup> The former consist of a polymeric material coated onto a substrate that is patterned by photolithography, laser ablation, or ion beam etching techniques. The pattern allows the transmission of light through the remaining polymer structure. Embedded waveguides use UV lithography to record a pattern onto a polymeric material by altering its chemical structure, thereby facilitating selective diffusion. Selective ion-diffusion of dye molecules can change the refractive index of the material.

The process requirements for waveguide materials exceed those found in many thermoplastics. A typical flip-chip configuration, in which the active chip area faces the substrate, is shown in Figure 2.3.2.2.1.<sup>122</sup> Materials used in this configuration need to withstand chip joining temperatures of up to 360°C, must be patternable to fit between C4 connections, need to allow signal detection by transmitting the information through the beveled plane reflector, and must not be influenced by organic solvents. Polyimides, which are well known for their excellent thermal stability, good dimensional stability, and high decomposition temperatures, can satisfy these material requirements.<sup>121</sup>

Polyimides that are thermally imidized from the polyamic acid were found to show large optical losses, which is inappropriate for the waveguide application. Upon polyamic acid cyclization to the polyimide and solvent removal, it was found that microvoids formed causing density fluctuations and light scattering leading to an optical loss in the material. On the other hand, fully imidized polyimides show a significant reduction in optical loss. By incorporation of bulky side groups, such as 6F and 3F, the polyimide can be used in the fully cyclized form.<sup>123</sup> The 6F and 3F groups also promote solubility, hinder chain ordering and chain transfer complexes, and give high  $T_g$  materials, all of which are favorable for this application.<sup>121</sup>

### 2.3.2.3 *Polyimides in Aerospace*

A number of structurally modified polyimides have been developed to meet the increasing demands of our societies' growing technology. The aerospace industry is one of those areas in which the material demands are ever increasing. Researchers have met this challenge primarily with polyimides, which can be modified to meet processing conditions while maintaining several of their advantageous properties.

Polyimides<sup>124-128</sup> are known to have excellent heat and chemical resistance, excellent adhesion to a number of substrates, and superior mechanical properties, such as high flexural modulus and compressive strength. Polyimides are also known to possess outstanding dimensional stability under loads, which allows their use in high temperature environments. The addition of phosphorus substituents is known to impart fire-retardancy as evidenced by high TGA char yields in air. Lee et al.<sup>127</sup> found that the

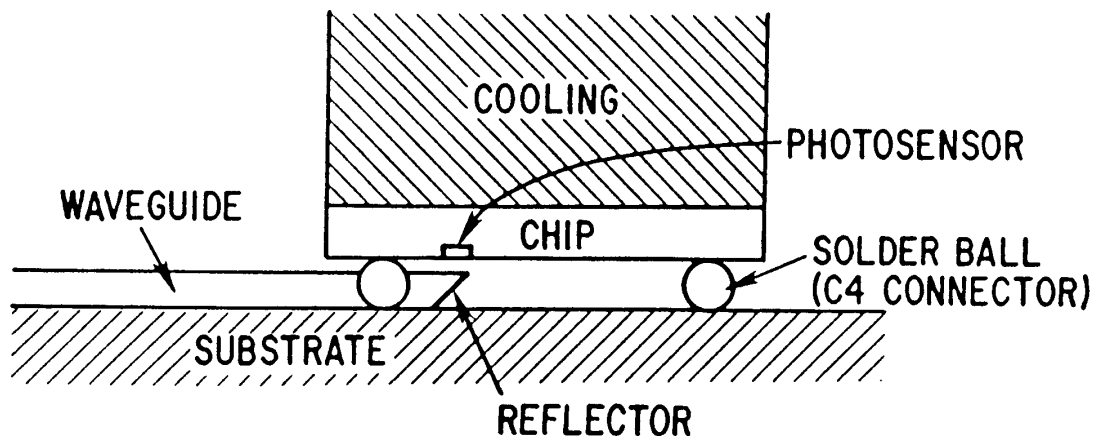


Figure 2.3.2.2.1 Flip-Chip Configuration with Waveguide<sup>122</sup>

incorporation of bis(*m*-amino phenoxy)triphenylphosphine oxide not only improved fire-retardancy but also solubility and adhesive strength to titanium.

The performance of polyimide composites surpasses that of mechanically fastened assemblies in terms of fatigue and corrosion resistance, aerodynamic properties, manufacturing costs, and repairs.<sup>124</sup> Due to these outstanding properties and economical advantages, polyimides are used in the aerospace industry as struts, brackets, composites, and structural adhesives.<sup>124-128</sup>

Composite applications, such as those found in aerospace, require the resin material to thoroughly wet the matrix, such as carbon fibers. In order to promote good wettability, the polyimide can be introduced as an oligomer. Oligomers, capped with reactive endgroups, exhibit lower melt viscosities and can undergo crosslinking at elevated temperatures. Commercial examples of these systems are shown in Table 2.3.2.3.1.<sup>128</sup> PMR-15 contains low molecular weight oligomers end-capped with nadic anhydride which undergo crosslinking at 250°C-300°C. The drawbacks of the PMR-15 is the volume of solvent removed such as methanol, water and cyclopentadiene, which produces voids in the final laminate. High temperature, void free systems can be achieved with acetylene, phenylacetylene, and phenylethynyl terminated oligomers.<sup>52,129-131,157</sup>

#### 2.3.2.4 *Polyimide Adhesives in Aerospace and Microelectronics*

Defining specific chemical interactions which lead to an adhesive bond has proven to be quite complex due to the number of variables involved. Several researchers have developed theories to explain and predict this type of interaction. The generally accepted theories of adhesion<sup>132-134</sup> are:

1. Mechanical Interlocking (or hooking): the adhesion is due to tortuous path of fracture

Table 2.3.2.3.1 Curable Polyimides for Aerospace Applications<sup>128, 302</sup>

<b>Monomers</b>	<b>Unsaturated end cap</b>	<b>Examples</b>
methylenedianiline, benzophenone dianhydride	nadic imide	PMR-15 LARC-13
methylenedianiline, maleic anhydride	maleimide	Kerimid 601
methylenedianiline, benzophenone dianhydride	phenylacetylene	ATPI Thermid
m-phenylene, bisphenol A dianhydride	phenylethynyl <sup>52,157</sup>	

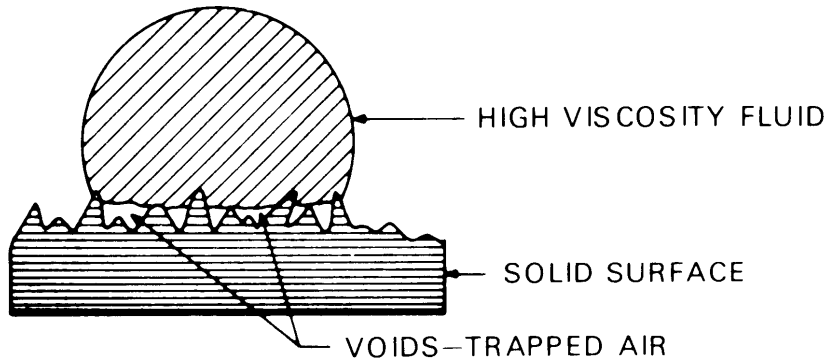
2. Surface Energetics: good wetting is required for good adhesion (Figure 2.3.2.4.1)<sup>135</sup>
3. Diffusion Theory: interpenetrating network formation occurs across the interface to form an interphase region
4. Acid-Base Theory: strength of the acid-base interaction affects adhesion strength
5. Chemical bonding: physical bond formation leads to adhesive strength
6. Weak Boundary Layer Mechanism: invoked to explain poor adhesion relating to cohesive failure in the interfacial region

It is impossible to explain adhesion by any one of these mechanisms, although one mode of adhesion may be predominant and lead to the majority of the observed adhesive strength.<sup>136,137</sup> The most desired interaction at the polymer/substrate interface is often proposed to be a chemical bond.<sup>138,139</sup> Unlike Van der Waals forces and hydrogen bonding, chemical bonds are much less likely to be disturbed by heat, water and exposure to chemicals.

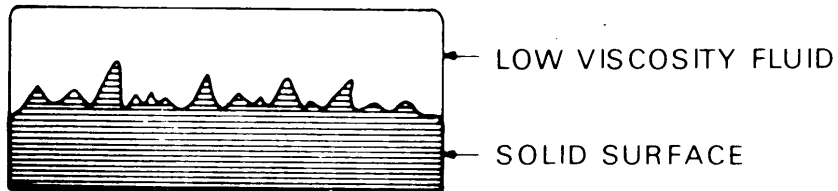
Surface contaminants will play a significant role in chemical interactions and bond durability and complicate the matter of adhesion,. Figure 2.3.2.4.2<sup>135</sup> depicts a typical surface with a number of adsorbed contaminants. It is essential to properly prepare the surface prior to polymer application. This can be done in a number of ways ranging from a pumice scrubber and heat treatments to reactive ion etching and chemical modification.<sup>140</sup>

Polyimide adhesives fall into one of three classes based on their adhesion characteristics.<sup>141,142</sup> The first class is amorphous polyimides, which self-adhere and bond well with metals such as Cu, Cr and Al. Semicrystalline polyimides form the second class of polyimide adherents. This class, in general, adheres well to reactive metals such as Al and Cr, but not to unreactive metals like Cu. Presumably, this is due to hindered





LOW AREA OF INTERFACIAL CONTACT RESULTING FROM HIGH VISCOSITY OF FLUID



LACK OF VOIDS AND HIGH AREA OF INTERFACIAL CONTACT RESULTING FROM LOW VISCOSITY OF FLUID

Figure 2.3.2.4.1 Effect of Adhesion Viscosity on Interfacial Contact<sup>135</sup>

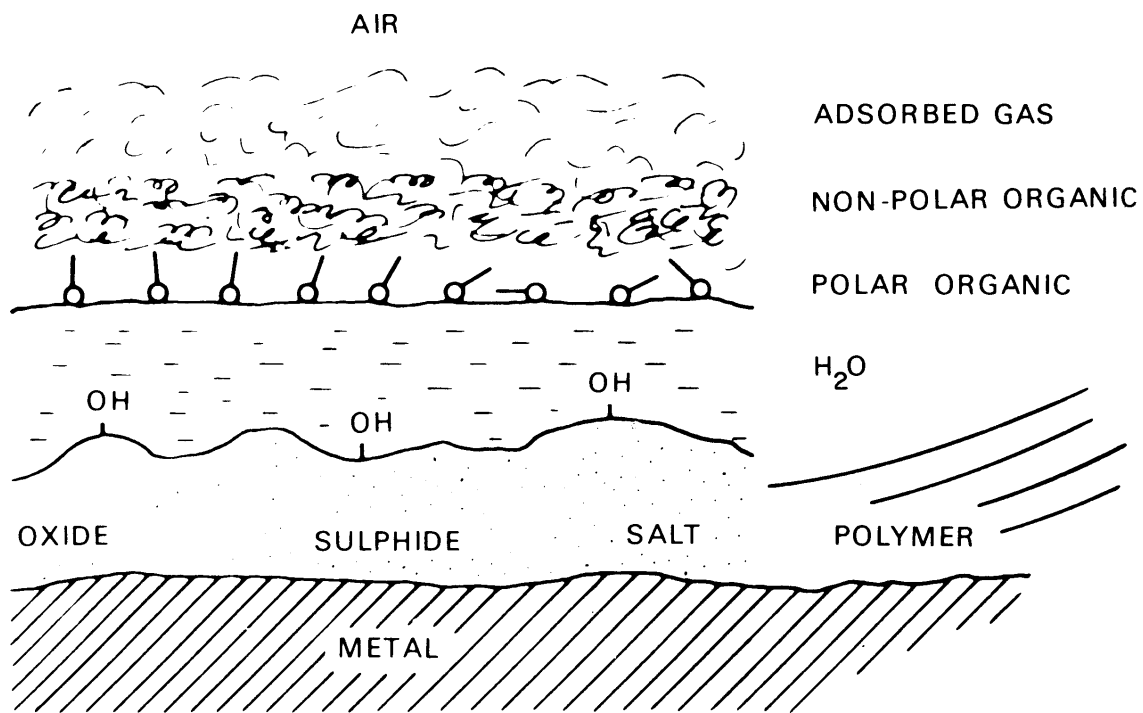


Figure 2.3.2.4.2 Hierarchy of Spontaneously Adsorbed Layers on a Metal Surface<sup>135</sup>

molecular mobility within the more ordered regions. Some semicrystalline polyimides also exhibit marginal self-adhesion. Brown et al.<sup>143</sup> showed that polyimide/polyimide adhesion is influenced by the cure temperature before adhesive bond formation. The bond strength between two fully cured (400°C) polyimides (ODA/PMDA) was weak whereas the bond strength between one fully cured polyimide with an incompletely cured polyimide (200°C) was good. The interdiffusion region between each set of polymer films was higher for the fully cured/incompletely cured laminent than it was for the fully cured/fully cured laminent (47nm vs. 30nm).<sup>143</sup>

Thermosetting resins represent a third class of polyimide adherents. Low molecular weight polyimides with curable endgroups allow for good wetting and adhere well to metals, ceramics and to themselves, if one of the layers remains uncured prior to adhesive bond formation.<sup>142</sup>

A number of geometries and test configurations can be used to determine material adhesive strength (Figure 2.3.2.4.3).<sup>132</sup> The adhesive strength values determined by each method in Figure 2.3.2.4.3 will vary with each methodology due to stress distributions in loaded adhesive joints generally being non-uniform.<sup>132</sup>

A structural adhesive is a bonding agent used for transferring required loads between adherents exposed to service environments typical for the structure involved.<sup>144</sup> Structural adhesives in aerospace applications need to withstand a number of extreme and dynamic environments ranging from radiation bombardment to reduced pressure ( $10^{-6}$ - $10^{-17}$  torr) and thermal cycling (-160°C to 120°C or -256°F to 248°F).<sup>145-150</sup> A missile in flight must be able to withstand a temperature of 500°C (932°F) for a few minutes and on aircraft for the high speed civil transport project must withstand temperatures ranging from 177°C to 232°C (351-450°F) for more than 50,000 hours. Truly, polymeric materials that satisfy these rigorous requirements qualify as “space-age” polymers.

Polyimides are leading candidates for aerospace applications<sup>4</sup> due to their excellent thermooxidative stability, good adhesion to metals and good mechanical properties over a wide range of temperatures. PMR-type chemistry (polymerization of monomeric reactants), which employs nadic anhydride endgroups, is a leading resin for this application (Scheme 2.3.2.4.1).<sup>151</sup> A potential drawback to using this material is the

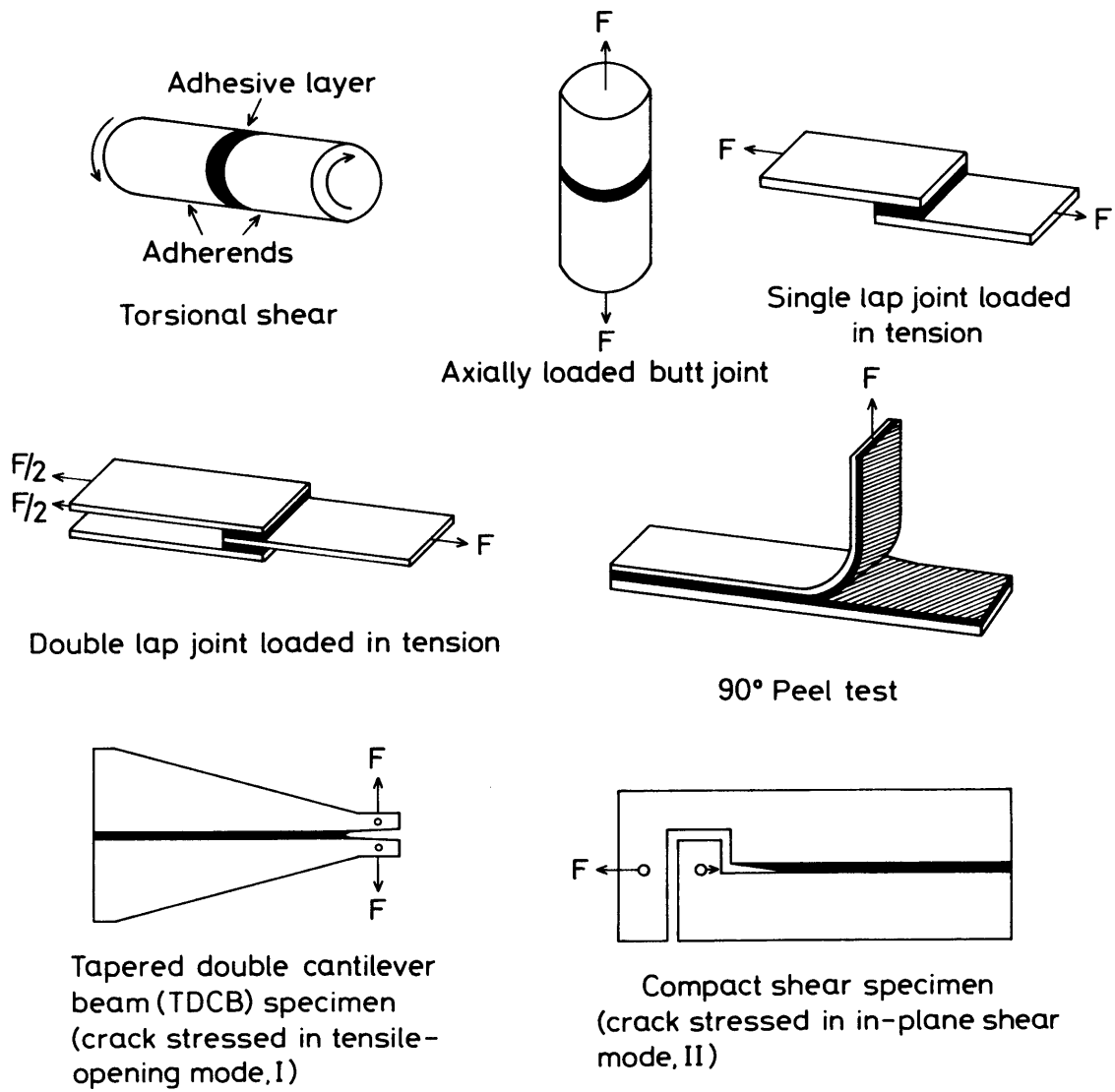
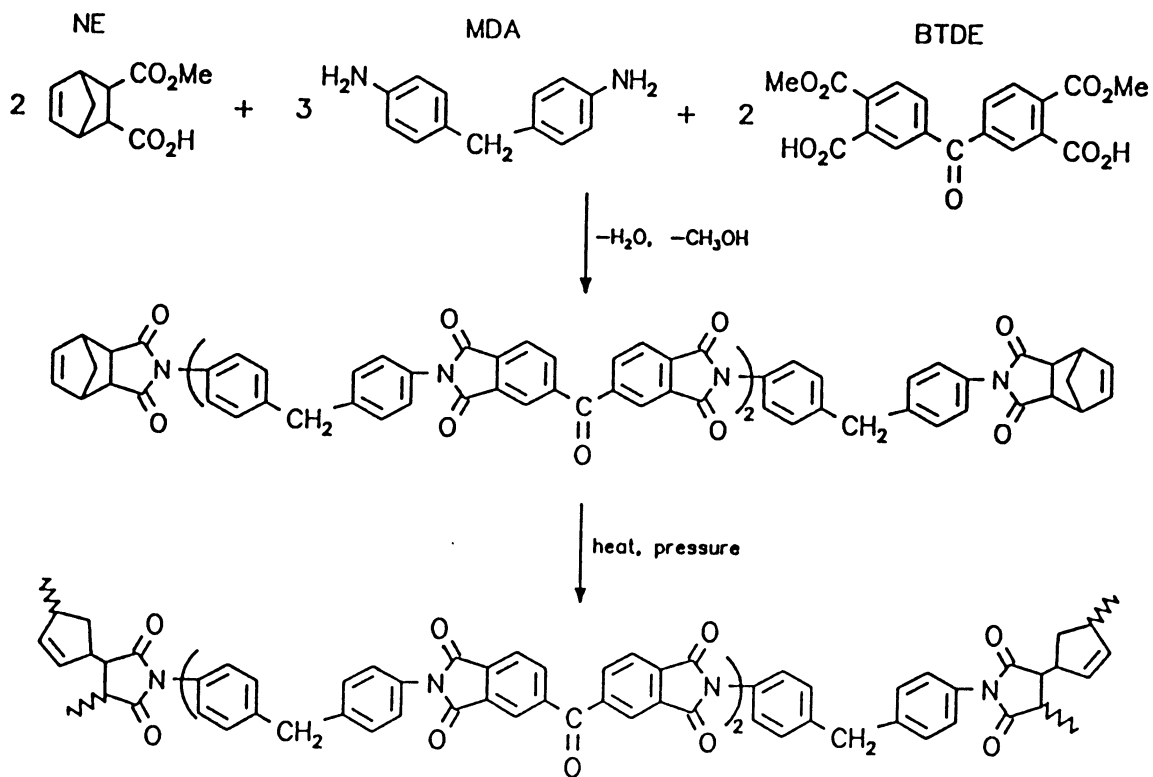


Figure 2.3.2.4.3 Sketches of Adhesive Joint Geometries<sup>132</sup>



Scheme 2.3.2.4.1 PMR-15 Resin Chemistry<sup>151</sup>

evolution of cyclopentadiene upon thermal crosslinking. Evolution of volatiles may produce a significant number of voids in the bondline,<sup>135</sup> which will reduce long-term adhesion.

The family of polyimide oligomers terminated with acetylene,<sup>131,152-154</sup> phenylacetylene<sup>156-158</sup>, phenylmaleimide<sup>129,159</sup> or phenylethynyl<sup>52,157</sup> reactive endcaps are alternatives to PMR-type chemistry. These materials, which may be fully cyclized, do not emit volatiles when thermally crosslinked at elevated temperatures and exhibit good adhesion to metals. They also have excellent shelflife, low crosslink density, excellent solvent resistance when cured, and wide processing windows between the glass transition temperature and cure exotherm (Figures 2.3.2.4.4 and 2.3.2.4.5).<sup>158</sup>

Microelectronic devices such as printed circuit boards and multichip packages also rely on good adhesion between polyimide-polyimide and polyimide-metal interfaces. For this application, polyimide precursors, either the polyamic acid (PAA) or polyamic ester (PAE), are generally applied to the desired substrate from solution to form a thin polymer layer, which can be imidized at elevated temperatures. This process involves a number of chemical and physical changes, many of which have not been sufficiently addressed due to the complexity of adhesive behavior.

Imidization of the PAA or PAE thin film results in loss of water, residual solvent and other volatile components present in the film. Because of the loss of volatiles and differences in the thermal coefficient of expansion between the film and substrate, the film experiences residual stress build-up.<sup>161,162</sup> Residual stress may lead to premature adhesive failure. The surrounding environment, such as humidity and temperature, in which the device operates will also affect the stress build-up<sup>163</sup> and bond stability.<sup>164</sup> Polyimides are known to absorb various amounts of water from their surroundings which may disrupt adhesion. This is illustrated by the common laboratory practice of applying water to remove polyimide films from glass substrates. Interfacial adhesion characteristics may be improved with coupling agents such as aminosilanes and aluminum chelates<sup>165</sup> (Figure 2.3.2.4.6).<sup>166</sup>

Ozawa and coworkers<sup>167</sup> reported data on a series of fully cyclized Probimide® photoimageable polyimides and compared them with PAA precursors of Kapton. These

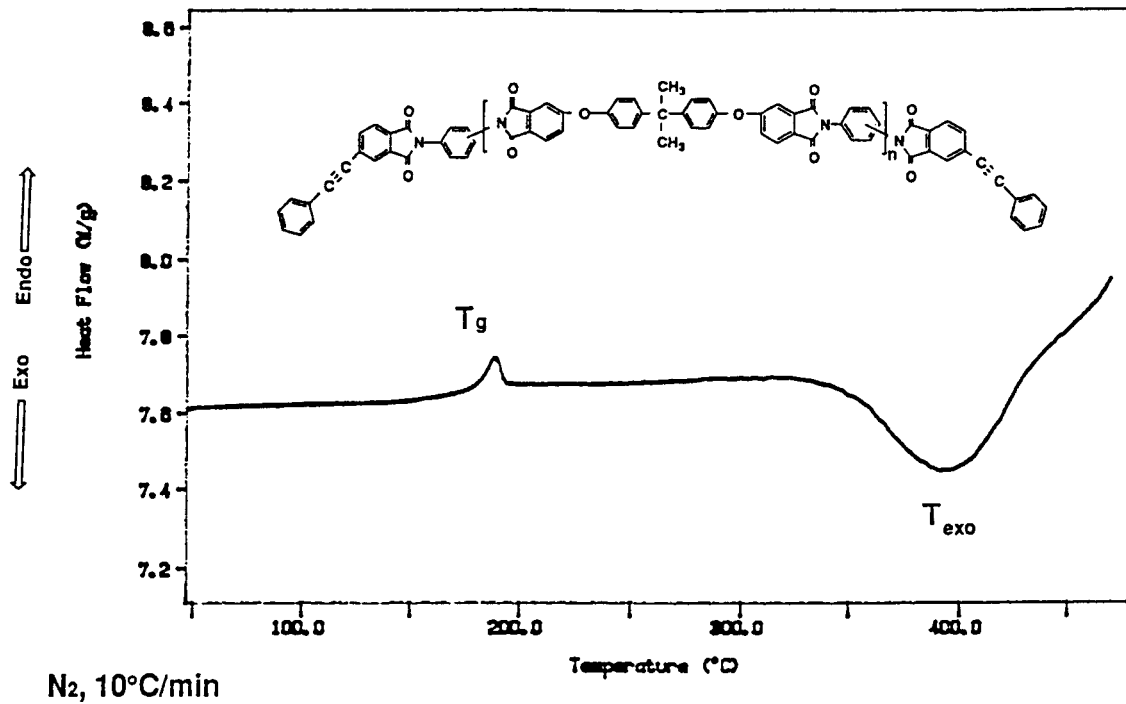


Figure 2.3.2.4.4 DSC Thermogram of Mn=3000 g/mol BPADA/m-PDA Phenyl Ethynyl Phthalic Anhydride Capped Polyetherimide Oligomers<sup>158</sup>

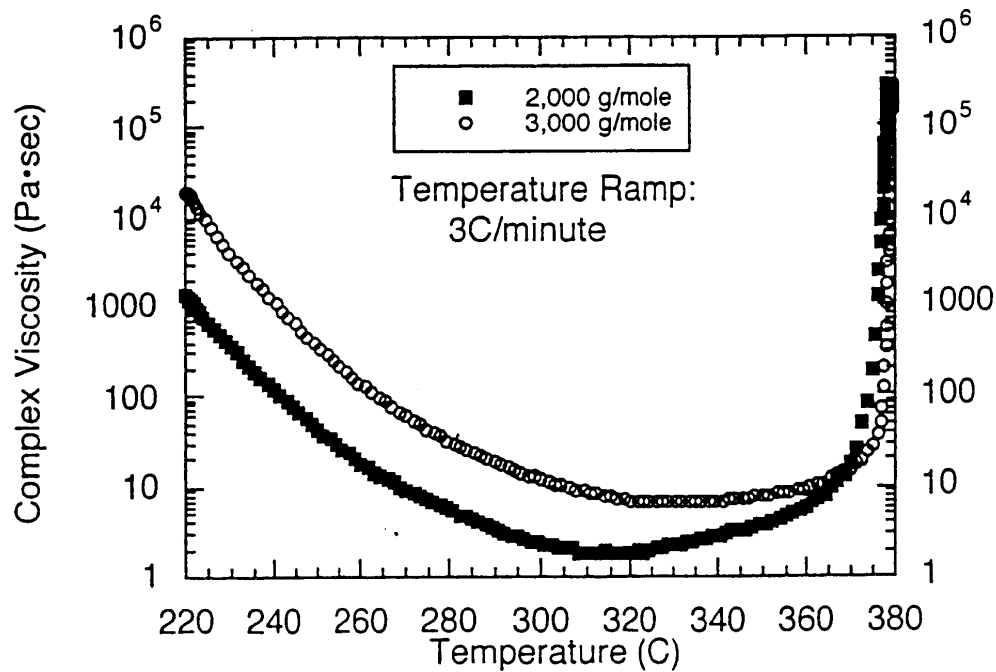


Figure 2.3.2.4.5 Rheological Characterization of BPADA/m-PDA Phenyl Ethynyl Phthalic Anhydride Capped Polyetherimide<sup>158</sup>

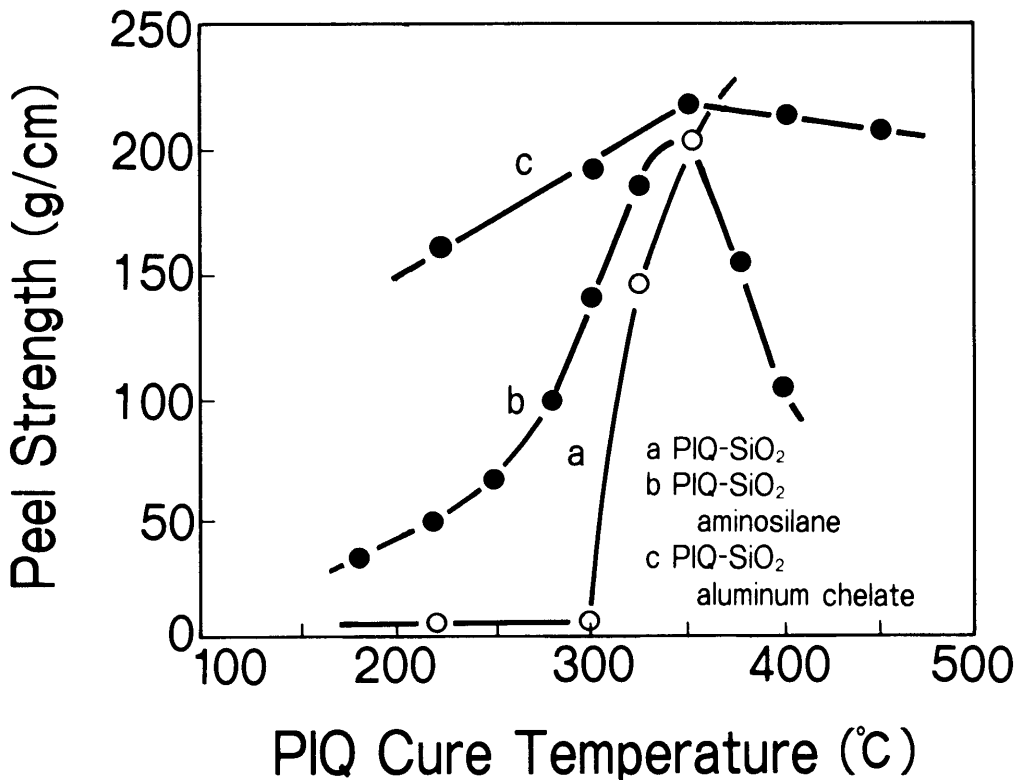
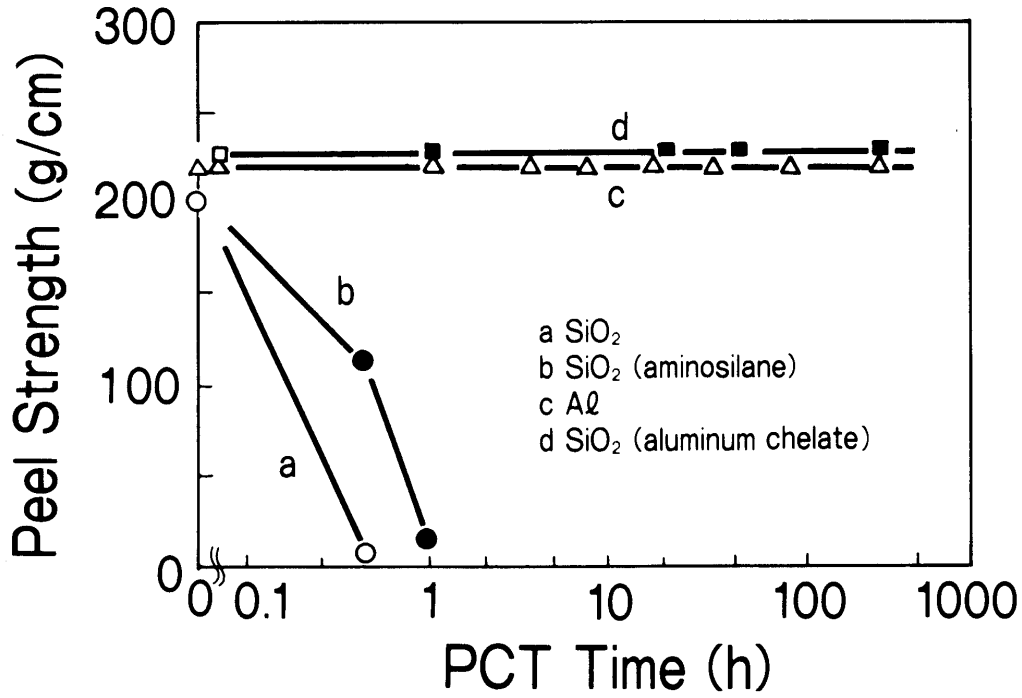


Figure 2.3.2.4.6 Adhesion Properties of PolyimideIsoindoloquinazolidione (PIQ) to SiO<sub>2</sub> with and without Adhesion Promoter (aminosilane)<sup>166</sup>



authors applied a typical cure schedule used in photolithography to each polymer, namely, 30 minutes at 110°C (soft bake) followed by 2-14 hours at 350°C (hard bake). Shrinkage of the polyamic acid materials ranged from 30-60% due to cyclization, which produces water, and residual solvent removal. The refractive index of the PAAs also changes dramatically upon conversion to the polyimide. On the other hand, the cyclized Probimide® series showed minimal shrinkage as well as constant refractive indices. Polymers, which maintain constant refractive indices and UV spectra over a wide range baking conditions, are useful for fabricating multilayered structures such as multichip modules.<sup>165</sup>

## 2.4 Gas Transport in Polymeric Membranes

This section will address the theory and physical description fundamental to the two methods for separating gas molecules. A brief description of gaseous diffusion through a porous membrane will be followed by an analogous treatment of dense films, including gas transport properties above and below  $T_g$ . The former is presented to illustrate the need for efficient and economic methods for separating gases.

### 2.4.1 Porous Membranes

Gas flow in porous membranes may be considered to be a competition between Knudsen flow and Poiseuille flow (Figure 2.4.1.1). Knudsen flow is favored if the membrane pore radius ( $r$ ) is less than the mean free path of the penetrant ( $\lambda$ ). Poiseuille flow exists when there are more collisions with other gas molecules than with the pore walls (e.g. a concentrated solution). If Poiseuille flow dominates, each of the gas molecules is coupled with another. Therefore, in the case of a bicomponent gas mixture, there will be no effective separation. The literature shows that poiseuille flow is predominant (>90%) when the ratio  $r/\lambda$  is greater than about 5.<sup>168</sup>

Porous membranes must operate in the Knudsen flow regime because when there is little or no separation of gas molecules occurring under Poiseuille flow conditions. When Knudsen flow governs the mode of separation, gas molecules are momentarily absorbed and then reflected in a random direction, resulting in few encounters with other gas molecules. Accordingly, the mean free path term is dominant. The mean free path is defined as

$$\lambda = (3\eta/2P) * (\pi RT/2M)^{1/2} \quad \text{Equation 1}$$

where  $M$ =gas molecular weight,  $P$ =pressure,  $\eta$ =viscosity of the gas,  $R$ =the universal gas constant, and  $T$ =temperature. As the gas molecules traverse the separating medium

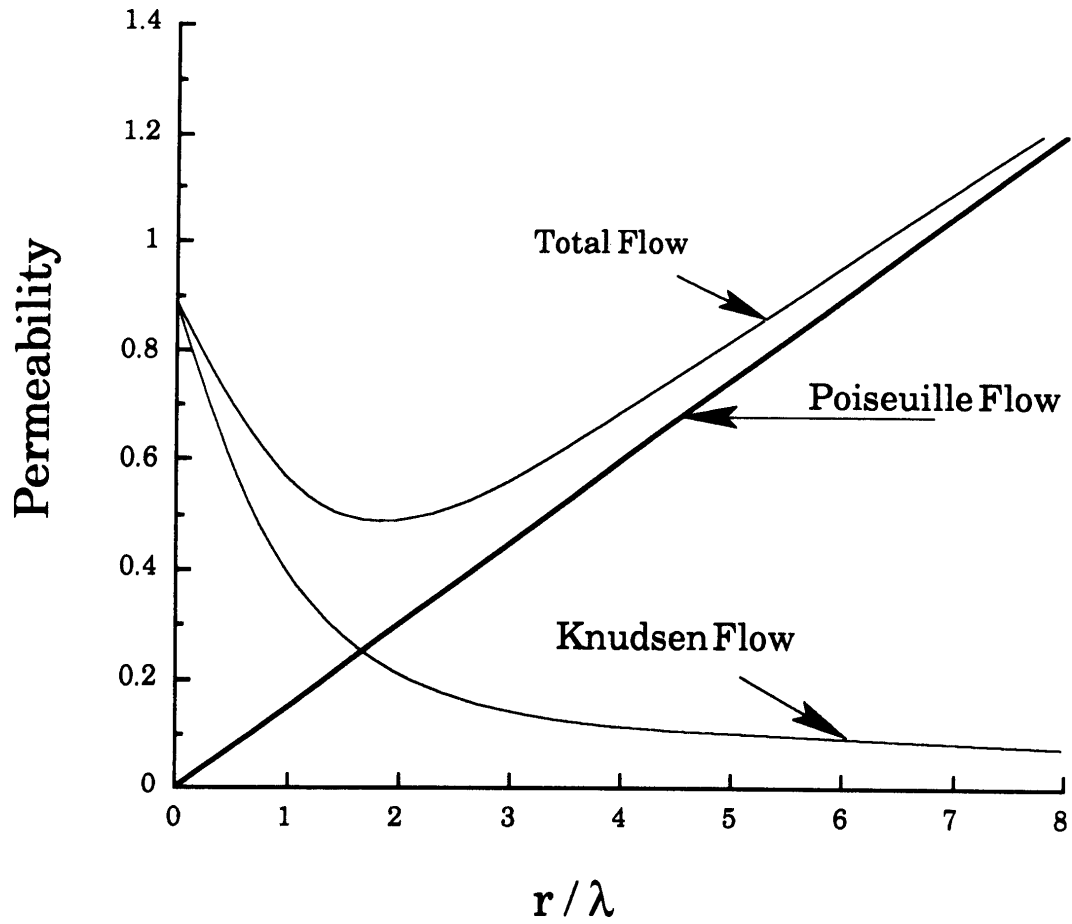


Figure 2.4.1.1 Total Flow in Porous Membranes Consists of Knudsen and Poiseuille Processes<sup>168</sup>

independently, they will reach a speed of travel called the mean molecular velocity,  $\mu$ , which is defined as

$$\mu = (8RT/\pi * M)^{1/2} \quad \text{Equation 2}$$

where R, T and M are as defined above. Equation 2 reveals that the mean molecular velocity is observed to be a function of molecular weight. In fact, the ideal separation factor for gases of different molecular weights is given by  $\alpha$ , the square root ratio of the molecular weights of the gases;

$$\alpha = [M_2/M_1]^{1/2} \quad \text{Equation 3}$$

where subscripts 1 and 2 denote gases of different molecular weights.<sup>169</sup>

Although Knudsen gas flow is used in some specialty applications,<sup>170,171</sup> its utility has been inherently limited due to the low gas concentrations required. A good example which demonstrates the magnitude of the energy and time required for separating molecules of similar molecular weights by Knudsen flow is given by Kesting and Fritzsche, who state that American diffusion plants utilized 10,276 stages for the separation of  $U^{235}F_6$  from  $U^{238}F_6$  because the separation factor for these molecules is 1.0043.<sup>168</sup> Thus, the inefficiency of Knudsen flow through porous membranes for separating large volumes of gases led to the development of dense membranes.

#### 2.4.2 Dense Membranes

Dense membranes have a significant advantage over porous membranes when applied to selective gas separation applications which is a direct result of the fundamental difference of penetrant/matrix interactions. As described above, the separation factor of porous membranes depends on the molecular weight ratio of the two gases. For dense

membranes, the separation depends on the difference in gas permeation which is a function of the particular physiochemical interactions experienced by each gas species within the polymer membrane.

The two major types of dense film membranes are: rubbery, which operate above their glass transition temperature ( $T_g$ ); and glassy, those which operate below their  $T_g$ . It has been noted that the mode of gaseous transport is quite different in the glassy state when compared to the rubbery state. This section will first focus on gas permeation behavior in rubbery materials, which will serve as a foundation for a similar treatment of glassy materials. Predictive techniques for gaseous transport in polymers will also be reviewed.

### **2.4.2.1 Rubbery Polymers (Elastomers)**

#### *2.4.2.1.1 Theory of Gas Permeation*

Rubbery polymers are capable of rubbery-type flow at temperatures above  $T_g$ . Recall that the  $T_g$  is the temperature interval where macromolecules experience increasing cooperative segmental motion along the backbone. Hence, elastomers above  $T_g$  have increased molecular motion as compared to glassy polymers.

Henry's Law (Equation 4) applies to elastomers permeated by low concentrations of supercritical gases (e.g.  $H_2$ ,  $O_2$ ,  $N_2$ ).<sup>172</sup>

$$\mathbf{C = S * p \quad \text{Equation 4}}$$

In Equation 4, C=the concentration of gas in the polymer (cc(STP)/cc polymer), S=Henry's solubility constant for a given gas/poly pair (cc(STP)/(cc polymer cmHg), and P=gas pressure in cmHg. Thus, the concentration of gas in the polymer increases with increasing gas pressure. It is interesting how this concentration changes across a membrane under applied pressure. Figure 2.4.2.1.1.1 depicts the process of a penetrant molecule migrating from the high-pressure interface to the low-pressure interface. The

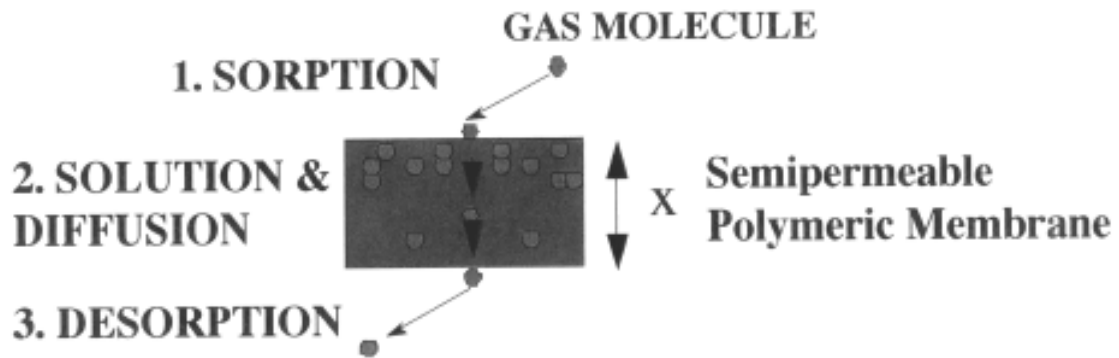


Figure 2.4.2.1.1.1 Gaseous Diffusion Across a Semipermeable Membrane

concentration of gas at any point in the membrane is given as  $(dC/dx)$ . Using this expression a total flux or rate of gas permeation,  $J$ , can be defined<sup>173</sup> as

$$\mathbf{J = D(dC/dx) = [cm^2/sec] \quad \text{Equation 5}}$$

where  $D$  is the diffusion coefficient. By integrating with respect to  $C$  and  $x$ , and utilizing Henry's Law, the more commonly known of the flux equation<sup>173</sup> can be developed (Equation 6).

$$\mathbf{J = P*(p_h-p_l)/x \quad \text{Equation 6}}$$

Here,  $P$ =permeability coefficient or permeability,  $p_h$ =gas pressure on the high-pressure side of the membrane,  $p_l$ =gas pressure on the low-pressure side of the membrane, and  $x$ =membrane thickness. The permeability coefficient is thus a product of the diffusion coefficient and the solubility constant (Equation 7).<sup>174</sup>

$$\mathbf{P = D*S \quad \text{Equation 7}}$$

This equation is frequently invoked for gas permeation through semipermeable membranes. Before proceeding any further it is worth defining the gas separation selectivity for a gas pair, which is as follows:

$$\mathbf{\alpha_{A/B} = P_A/P_B = [D_A/D_B]*[S_A/S_B] \quad \text{Equation 8}}$$

where  $\alpha_{A/B}$  is the ratio of the permeability of gas A to gas B.<sup>174</sup> A diffusive and solubility selectivity can also be defined as  $[D_A/D_B]$  and  $[S_A/S_B]$ , respectively. In the literature, it is common to report the permeability of a particular gas through a polymer membrane, as well as the membrane's selectivity with regard to that gas in the bicomponent mixture.

Clearly, it would be desirable to combine both a high selectivity and a high permeability for a single polymer, since that would allow one to obtain large volumes of pure gas.

Permeability is the product of the diffusion coefficient and the solubility constant. The temperature dependence of these parameters is an important issue. It has been found that each of these parameters have the following dependence on temperature,<sup>168</sup>

$$D = D_0 * e^{-E(D)/RT} \quad \text{Equation 9}$$

$$P = P_0 * e^{-E(P)/RT} \quad \text{Equation 10}$$

$$S = S_0 * e^{-\Delta H(S)/RT} \quad \text{Equation 11}$$

where  $E_d=(E(D))$ =apparent activation energy of the diffusion process,  $E_p=(E(P))$ =apparent activation energy of the permeation process,  $\Delta H_s=(\Delta H(S))$ =molar heat (enthalpy) of solution, and  $P_0$ ,  $D_0$ , and  $S_0$  are preexponential factors. Combining Equations 9-11 allows one to define Equation 12, as follows:

$$E_p = E_d + \Delta H_s \quad \text{Equation 12}$$

where  $E_p$  depends on the magnitude of  $E_d$  and  $\Delta H_s$ .  $E_d$  is always positive and therefore the diffusion always increases with temperature. The thermodynamic parameter  $\Delta H_s$ , on the other hand, can be positive or negative, depending on the polymer-gas interactions.<sup>172</sup> The apparent activation energy of permeation is therefore a function of the specific polymer gas interaction.

#### 2.4.2.1.2 A Physical Description of Gas Permeation



Thomas Graham postulated a mechanism in 1866 for the transport of gas molecules through a semipermeable membrane.<sup>175</sup> This mechanism contains three steps: the solution of the gas flows onto the upstream (high-pressure) surface of the membrane, gas diffuses through the membrane, and finally, gas evaporates from the downstream (low-pressure) surface of the membrane. This early description of gaseous transport is considered to be the basis for today's "solution-diffusion model", which is used to explain many membrane separations.<sup>176</sup>

The solution and evaporation processes at either face of the membrane take place much more rapidly than does the gas transport through the membrane. The rate-determining step of the overall process is gas permeation through the membrane. Permeation is a function of two parameters: the solubility constant,  $S$ , and the diffusion coefficient,  $D$ . The solubility constant is a thermodynamic term based on the specific polymer-penetrant interactions and the condensibility of the penetrant, and the diffusion coefficient is a kinetic term referring to the movement of gas molecules inside the polymer matrix.<sup>174</sup> Although there is ongoing discussion with regard to what the polymer chains are actually doing, there is general agreement that the chains are sufficiently perturbed during this process to allow a penetrant molecule to reside between chains. The migration of gas molecules diffusing across the membrane requires energy in order to develop a location in the membrane downstream that is dimensionally favorable for the gas molecule. Stated another way, the diffusion coefficient determines "how frequently, on a time-averaged basis, a hole of sufficient volume appears next to the gas penetrant, enabling it to jump further through the membrane".<sup>168</sup> From this description of molecular diffusion it can easily be seen that an increase in chain backbone rigidity and/or intersegmental packing, which leads to a tighter structure and hindered bond rotation, will decrease the diffusion coefficient.<sup>177</sup>

A rubbery polymer functioning as the gas-separating medium under Henry Law conditions, where both  $S$  and  $D$  are constants,<sup>172</sup> can be relatively easy to describe compared to the transport of penetrants through a non-equilibrium state glassy polymer. Differences in the two states will be addressed in the following sections.

## 2.4.2.2 Glassy Polymers

### 2.4.2.2.1 Theory of Gas Permeation

The process of gaseous diffusion in glassy polymers is known to be more complex than that of rubbery polymers. The reason lies in the inhomogeneity which is due to “intersegmental packing defects frozen into the structure” when the temperature drops below the  $T_g$ .<sup>168</sup> The heterogeneity of glassy polymers result in deviations from Henry’s Law with respect to linear dependence of concentration versus applied pressure. Two types of sorption sites have been introduced to account for this non-linearity.<sup>178</sup> The first is called “Henry’s site” and the second is known as “Langmuir’s site”. Molecules in a Henry-type site obey Henry’s law and reside in the normally densified regions of the polymer. Molecules in a Langmuir-type site do not obey Henry’s law and reside either in microvoids (excess free volume frozen into the matrix) or “any mechanism which immobilizes penetrant molecules in a heterogeneous medium”.<sup>179</sup> Molecules in these sites are much less mobile than the ones in Henry-type sites. Local equilibrium exists between molecules in Henry and Langmuir sites. The description of gas sorption and diffusion through glassy polymers utilizing two different sites has become known as the “dual-mode sorption theory”.<sup>180</sup>

Since solubility can either occur in Langmuir sites,  $C_H$ , or Henry sites,  $C_D$ , the overall solubility now becomes

$$C = C_D + C_H \quad \text{Equation 13}$$

where  $C$  is the total solubility. A molecule in a Henry site obeys solubility as defined by Equation 14, but the solubility of a molecule in a Langmuir site shows a non-linear dependence on pressure, as shown in Equation 15

$$C_D = S \cdot p \quad \text{Equation 14}$$

$$C_H = [C'_H * b * p] / [1 + b * p] \quad \text{Equation 15}$$

where  $C'_H$  = the hole saturation constant (a measure of sorption capacity) and  $b$  = characterizes the tendency for a penetrant to sorb into the Langmuir site (' $b$ ' is lower for smaller molecules). Therefore, for glassy polymers the solubility is no longer a constant but a function of pressure, penetrant size, and the concentration of Langmuir sites.

If Henry's law conditions are not met, as in the case for glassy systems, the diffusion coefficient is no longer constant but becomes a function of thermal history and position in the membrane.<sup>181,182</sup> Others have extended this theory by noting that sorbed penetrants in Langmuir sites may not be totally immobilized.<sup>183-185</sup> This is still an active area of research<sup>186</sup> and has been called the "dual-mode transport theory".<sup>187-189</sup>

#### 2.4.2.2.2 *A Physical Description of Gas Permeation*

The mechanisms for gas transport through glassy polymers are incompletely understood when considered on a molecular level. This is partially due to the inability to investigate individual molecules as they traverse the matrix. Although significant progress has been made in defining some mechanisms which describe penetrant passage, these models apply to only a select number of polymer/gas systems.<sup>172</sup> As a result, a number of statistical models have been developed to explain the transport mechanism and estimate the parameters  $P$ ,  $D$  and  $S$ .<sup>190,191</sup> Most of the theoretical transport models found in the literature contain one or more adjustable parameters which are experimentally obtained.<sup>172</sup> Additionally, expressions for gas diffusion coefficients, permeability coefficients and activation energies have been derived from "free-volume, statistical-mechanical, energetic, structural, or other considerations".<sup>172</sup> Some of these models/derivations are described in references 182,192-196. One of the most popular concepts for modeling gas permeation is based on the available free-volume or "empty" volume of the system, which can be related to the penetrant concentration in the matrix.<sup>197-200</sup> This type of model suggests that gas permeability not only varies with free-

volume, which can be estimated by group contribution methods,<sup>201,202</sup> but also with the free-volume distribution, which until now has been difficult to ascertain. Recently, macromolecular structure has been successfully probed using positron annihilation to determine the free-volume distribution.<sup>203,204</sup> In the future, it would be quite instructive to compare this experimental data with that obtained from computer simulated calculations of the free-volume distribution.

### 2.4.3 Predictive Techniques for Gaseous Transport in Polymers

#### 2.4.3.1 Empirical Correlations

A body of experimental data on gaseous diffusion through polymeric membranes has become available over the past several decades. Salame, a pioneer in this area, has developed a method for correlating this data through group contributions to permeability.<sup>205,206</sup> He has defined a method which involves a parameter called a permachor ( $\pi$ ) defined as

$$\pi = -(2.3/S) * \log (P/P^*) \text{ Equation 16}$$

where  $P^*$  is permeability of  $N_2$  in natural rubber,  $P$  is permeability of  $N_2$  in the test polymer, and  $S$  is the scaling factor. Salame and others have been moderately successful in predicting trends in polymer permeabilities. However, polymers that have been projected to be identical with respect to oxygen permeation were also predicted to have equal selectivity when using Salame's method.<sup>207</sup>

More recently, Park and Paul have correlated this data by using an empirical modification of a free volume scheme.<sup>208</sup> Unlike the permachor calculations, their method does not require a scaling factor which incorporates an experimental density or an estimate of the occupied volume from a group contribution method. This new method may significantly improve the accuracy predicting and correlating gas transport properties of glassy polymer membranes.<sup>208</sup>

Robeson et al.<sup>209</sup> has derived a procedure for predicting gas permeation behavior for aromatic polymers, such as polysulfones, polycarbonates, polyarylates, poly(aryl ketones) and poly(aryl ethers), which utilizes Equation 7,

$$\ln P = \sum_{i=1}^n (\phi_i \ln P_i) \quad \text{Equation 17}$$

where P=permeability,  $\phi_i$ =volume fraction of a structural unit  $i$  and  $P_i$ =the permeability contribution of the structural unit. Using existing data and Equation 17, solutions can be generated for a particular system by using a least squares fit. The molar volume contributions can be calculated using a computer software program. Excellent agreement between predicted and experimental values for P have been reported.<sup>210</sup> In the future, this technique will be extended to other systems, such as polyamides and polyimides.<sup>209</sup>

#### *2.4.3.2 Molecular Modeling via Computer Simulations*

Computer simulation is a key to discovering a wealth of useful knowledge for many disciplines. As a really extreme example, Hawkings, a well known astrophysicist, has dedicated his life to developing the Unification Theory which he believes will allow him and others to predict the outcome of future events based on an accurate and detailed historical record.<sup>211</sup>

Currently, there is no widely accepted method for predicting gas-selecting properties beyond that of applying previously determined trends or estimates based on subsegment contributions. In gas permeation science, the “holy grail” or key to unlocking total structure/property relationships, is computer-aided molecular modeling which attempts to probe specific motions of both the penetrant and matrix using the known intra- and intermolecular forces of each.<sup>194</sup>

The earlier computer aided descriptions of gas transport processes predicted diffusion coefficients and the activation energies for diffusion.<sup>196,212</sup> More recently, advances in computer simulations have shed greater light on the overall transport process individual penetrants. The following section will present some of the more recent

advances in this area, in which more progress has been made for rubbery polymers than for glassy polymers. This is due to the relatively longer computational time needed to simulate the non-equilibrium thermodynamic state intrinsic to diffusion through a glassy system.

#### ***2.4.3.3 Recent Advances in Molecular Modeling***

The area of computer simulated modeling of gaseous transport through dense membranes is very new. The first reported work is attributed to Shah et al. in 1989 in which he and coworkers estimated the fractional free volume available to spherical penetrants within polypropylene and poly(vinyl chloride) matrices.<sup>213</sup> Since 1989, significant discoveries have been made using molecular dynamic simulations on several structurally “simple” polymers (e.g. polyethylene,<sup>214,215</sup> atactic polypropylene<sup>216,217</sup> and polyisobutylene<sup>218,219</sup>) as well as on more “complicated” ones such as polycarbonate,<sup>220</sup> polystyrene,<sup>221</sup> and polyimides.<sup>222,223</sup>

During 1990, Takeuchi utilized molecular dynamic simulations to show the migration path (or “jump”) of an oxygen molecule through a glassy -CH<sub>2</sub>- matrix. The simulation was based on migration from one low energy site to another through a channel, which required an energy of activation (Figure 2.4.3.3.1).<sup>224</sup> Similarly, Smit et al. in 1992 described a similar movement of CO<sub>2</sub> through a polyimide systems (Figure 2.4.3.3.2).<sup>223</sup> In both of these examples, a channel is initially formed which lowers the energy barrier for migration. Afterward, the channel collapses and traps the penetrant in a new cavity.<sup>224</sup> These two examples, as well as many others, strongly suggest that part of the gas diffusion mechanism consists of molecules “jumping” successively through lower energy sites within the polymer matrix.

Zhang et al. published some insightful work in 1995 based on molecular dynamic simulations for a polyimide interacting with O<sub>2</sub> and N<sub>2</sub> in the bulk.<sup>222</sup> The simulations enabled determination of the number of times O<sub>2</sub> interacted with different functional sites on the polymer backbone. Although this approach needs to be further developed, it has

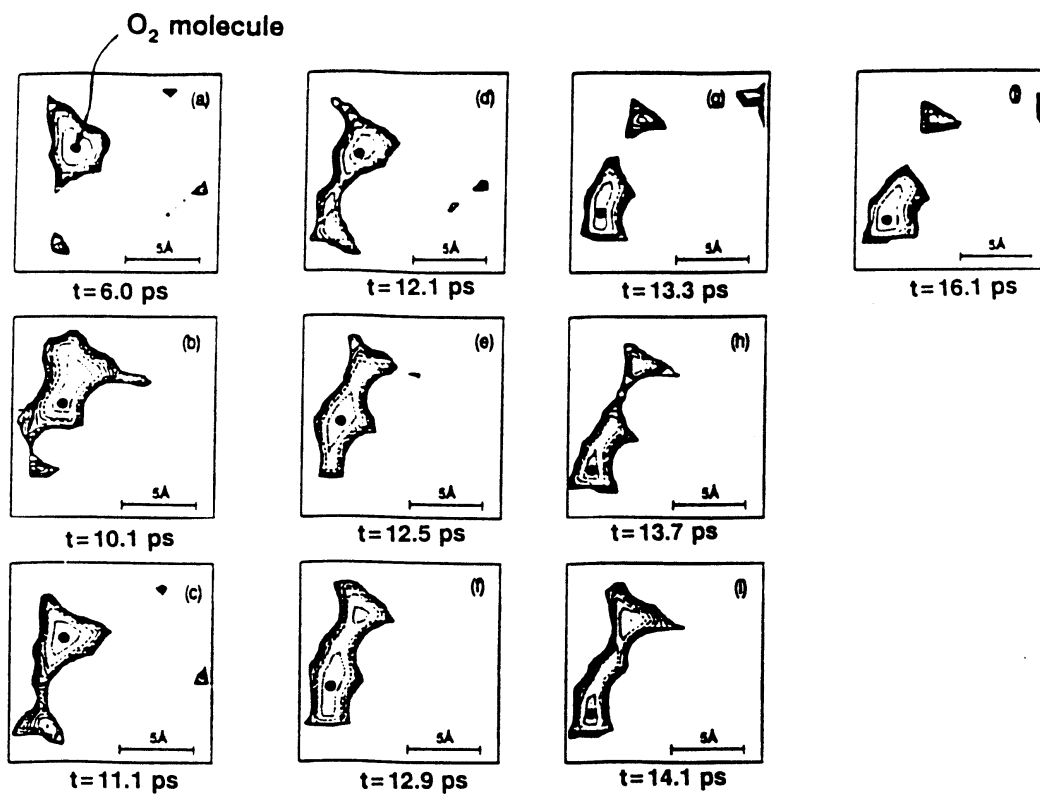


Figure 2.4.3.3.1 Molecular Dynamic Simulations of a "Jump" of an  $O_2$  Molecule in a Glassy  $-CH_2-$  Matrix. Changes in the Potential Energy Surfaces of "Cages" Enclosing the Penetrant Molecule<sup>224</sup>

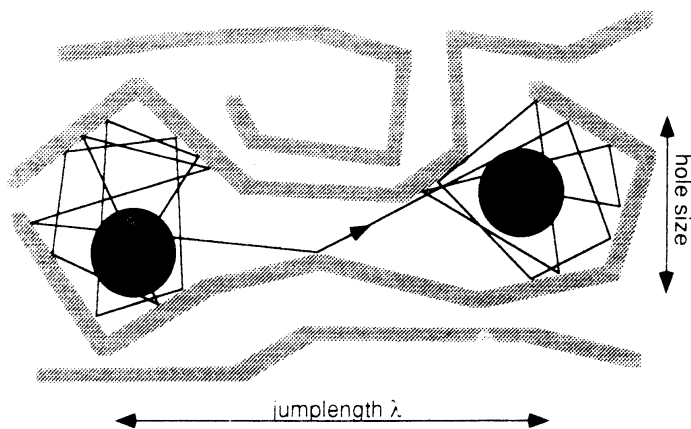
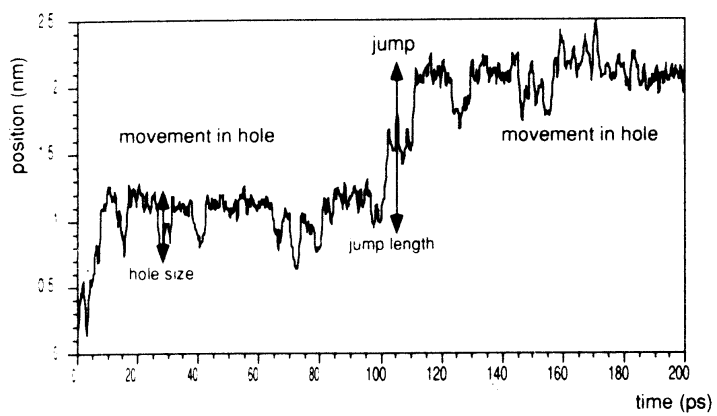


Figure 2.4.3.3.2 Movement and “Jump” of CO<sub>2</sub> Molecules Inside the Matrix of 6FDA-4,4’-PDA Polyimide<sup>223</sup>



the exciting possibility of elucidating specific interaction of gas penetrants throughout a polymeric system.

There is also an ongoing search for estimation methods that do not require large amounts of computer time. One example is the multidimensional transition state theory (TST) which studies the elementary jumps needed for a penetrant to traverse a glassy polymer.<sup>225,226</sup> This approach “determines spatial fluctuations in the accessible volume for a particular penetrant” and uses these fluctuations to determine the adjustable parameters in the transition state theory.<sup>227</sup> This method has the advantage of ignoring “nonjump” motions, thereby simplifying calculations and reducing the amount of computational time.<sup>226</sup>

For other examples of computer simulated modeling of gaseous transport, or computer simulations in general, see References 228-230.

#### ***2.4.3.4 The Current State of the Art***

Since the 1960's, membrane separation of gases has progressed from being merely a laboratory curiosity to serving a large scale commercial need for purified gases. From this beginning until the early 1990's, hundreds of permeation measurements have been reported for a number of important polymer structures from aliphatic rubbers to glassy aromatic materials.

In 1991, Robeson<sup>231</sup> reported trends that he found to be applicable to all permeation measurements. He observed that, regardless of the repeat unit, polymer gas transport properties did not exceed a certain boundary level when viewed on a  $\log(\alpha_{A/B})$  versus  $\log(P_A)$  plot, where A is the faster permeating gas. This boundary is defined as the “upper bound”, which is the upper limit of gas separation performance for current state of the art membranes (Figure 2.4.3.4.1).<sup>231</sup> As membrane technology improves, it is likely that this bound will shift further upward.

Robeson also investigated the respective contributions of D and S to P.<sup>231</sup> Figures 2.4.3.4.2 and 2.4.3.4.3 show plots of  $S_{He}/S_{N_2}$  and  $D_{He}/D_{N_2}$ , the product of which is  $P_{He}/P_{N_2}$ . (Equation 18)

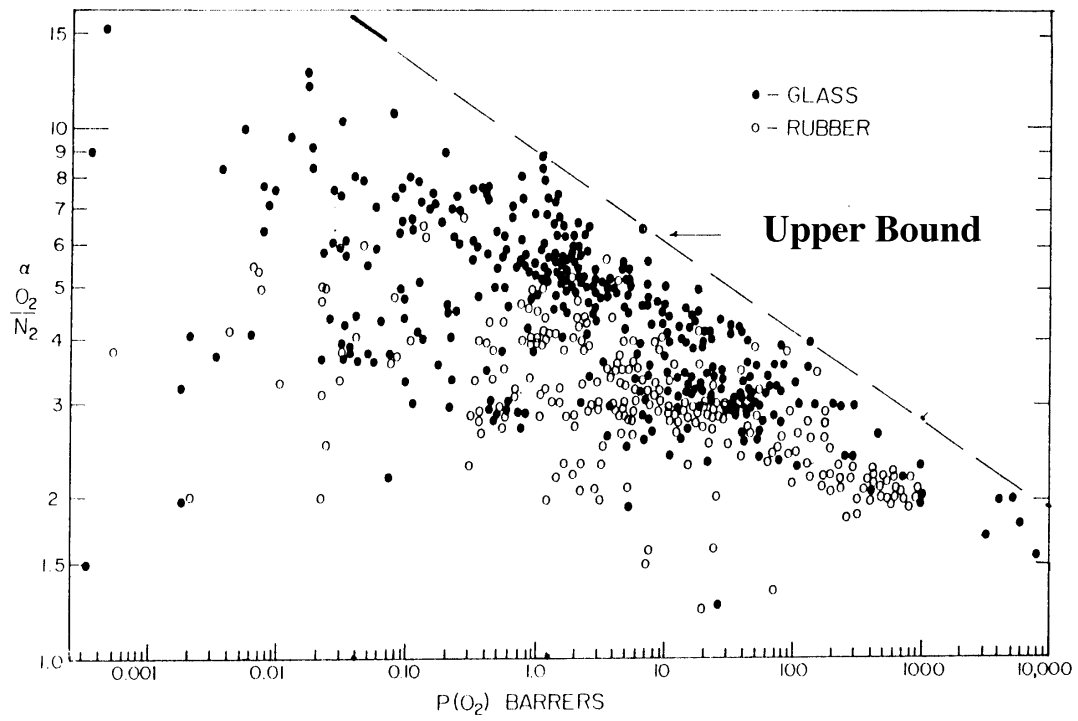


Figure 2.4.3.4.1  $\text{Log}(\alpha(\text{O}_2/\text{N}_2))$  vs.  $\text{Log}(P(\text{O}_2))$ . The Current State of the Art Polymers for Gas Selectivity Defines an Upper-Bound<sup>231</sup>

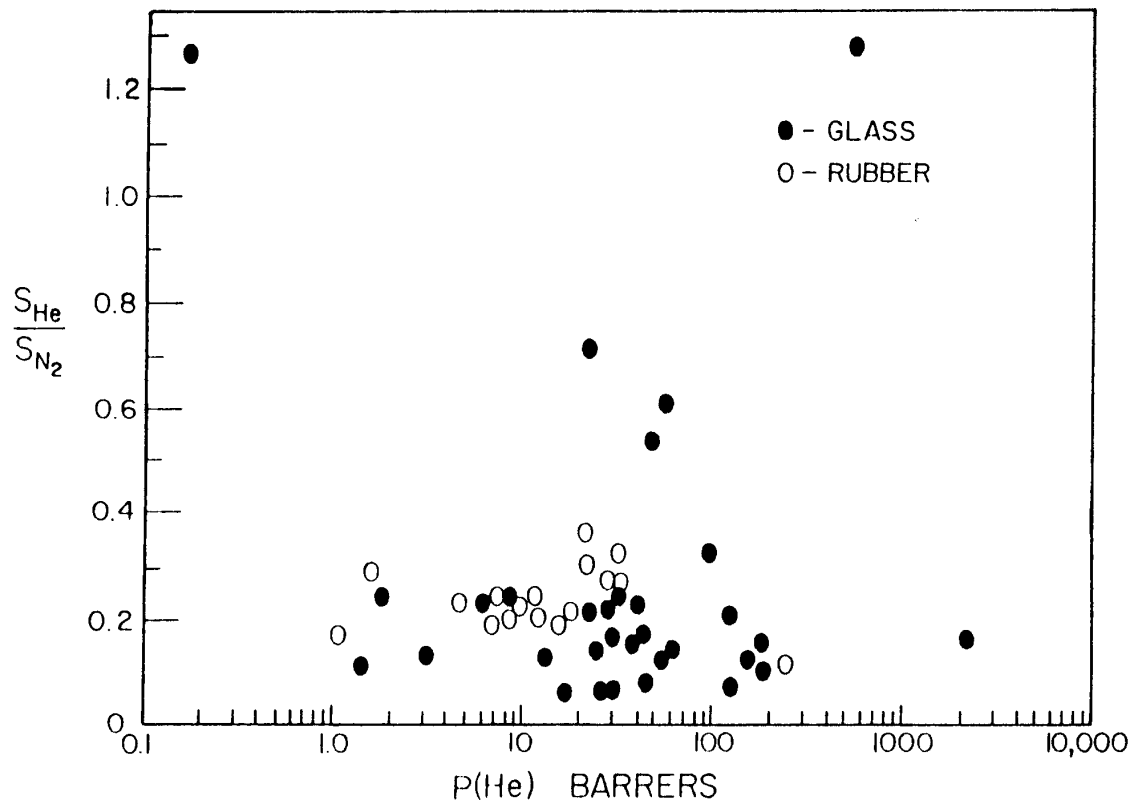


Figure 2.4.3.4.2  $S_{He}/S_{N_2}$  vs.  $\text{Log}(P_{He})^{231}$

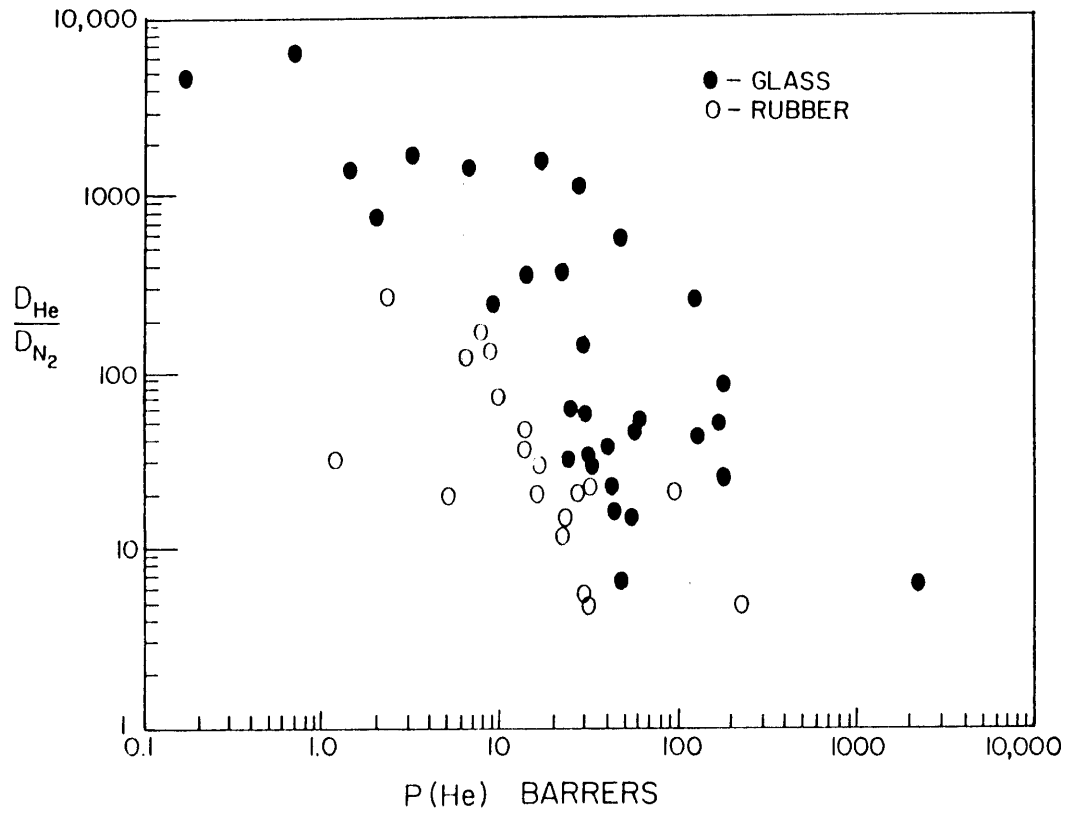


Figure 2.4.3.4.3 Log (D<sub>He</sub>/D<sub>N(2)</sub>) vs. Log (P<sub>He</sub>)<sup>231</sup>

$$\alpha = P_{\text{He}}/P_{\text{N}_2} = (D_{\text{He}}/D_{\text{N}_2}) \cdot (S_{\text{He}}/S_{\text{N}_2}) \quad \text{Equation 18}$$

The solubility constant ratio as plotted against  $P_{\text{He}}$  shows very little variation, ranging from 0.05-0.35 for the majority of the data points. The few points having a ratio greater than 1.2 are most likely due to anomalous behavior.<sup>231</sup> In comparison, the plot of  $D_{\text{He}}/D_{\text{N}_2}$  versus  $P_{\text{He}}$  shows a wide range of values from 5-7,000. This illustrates that the primary factor contributing to the overall permeability selectivity is the diffusive selectivity. This is also true for many other gas pairs in addition to He/N<sub>2</sub>.

## 2.5 Structure-Property Relationships in Selective Gas Separation

A major objective in macromolecular science is to properly design and optimize the polymeric repeat unit, since this allows one to selectively tailor certain material properties. The relationship between the microscopic and macroscopic properties of a material is also called the “structure-property” relationship. Gas permeation science investigates inter- and intra-chain interactions of the polymer with respect to penetration by gas molecules, and on the microscopic level it is a sensitive probe to slight modifications in molecular structure.

There is a general relationship reported in the literature that as the permeability of gas A increases, its selectivity decreases.<sup>232</sup> This behavior is easily understood if the matrix is capable of tightly packing since the free volume, or unoccupied space, is reduced thereby decreasing its ability to transport permeants. Concurrently, the same material shows an improved “sieving” or higher selecting ability between gases of different sizes, shapes and electronic environments. While this general trend is true of polyimides, as well as most other polymers, there is a continuing goal to synthesize materials which can simultaneously achieve both higher permeability and higher selectivity, or which can attain higher permeability with only a slight reduction in selectivity. Two criteria have emerged to guide synthetic researchers in improving the permselectivity of membranes,<sup>233-236</sup> which have evolved through extensive experimentation:

1. inhibition of intersegmental packing while simultaneously inhibiting intrasegmental (backbone) mobility
2. weakening interchain interactions (reduction of charge transfer complexes)

A proper application of these two principles may lead to membrane permselectivity above that defined by Robeson's concept of "upper bound".<sup>231</sup> This chapter reviews methods that have been employed which incorporate these principles.

### 2.5.1 Repeat Unit Design to Increase Permeability and Selectivity

Polyimides containing a  $-C(CF_3)_2-$  link ('6F') in the repeat unit (eg. 6FDA) have been found, in many cases, to increase both the selectivity and permeability.<sup>237,238</sup> Three primary reasons why this is true have been suggested.<sup>239</sup> Incorporation of a large bulky group into the backbone inhibits the intrasegmental mobility due to the greater energy needed to rotate around the Ph-C bond, which is sterically hindered by the Ph-H/ $CF_3$  interaction (Figure 2.5.1.1). Not only do the '6F' groups increase chain stiffness, but they also act as molecular spacers to decrease chain packing, resulting in a polymer with greater free volume. Finally, as a result of reduced chain packing, the tendency to form charge transfer complexes (CTCs) is weakened or even eliminated. A decrease in CTCs increases the permeability and can be visually detected by the disappearance of color.<sup>240</sup> Dianhydrides incorporating '6F' are generally more effective at enhancing selectivity versus comparable diamines containing '6F' groups. A dianhydride which has been found to behave similar to 6FDA, called bis(phenylcarboxylic dianhydride) dimethylsilane, has been shown to increase permeability without significantly decreasing selectivity.<sup>241</sup>

Pendant alkyl groups<sup>242,243</sup> have also shown the ability to restrict intramolecular rotation while maintaining a highly rigid structure (Table 2.5.1.1).<sup>242</sup> Interestingly, the solubility selectivities for these materials remain relatively constant (1.2-1.3), while the range in the diffusive selectivities is quite wide, from 2.7 to 5.0. It is also evident that by increasing the bulkiness of the diamine with an increasing number of methyl substituents, the diffusive selectivities decrease as a result of greater free volume. In this case, although the permeability increases with each methyl substituent, the selectivity is reduced considerably.

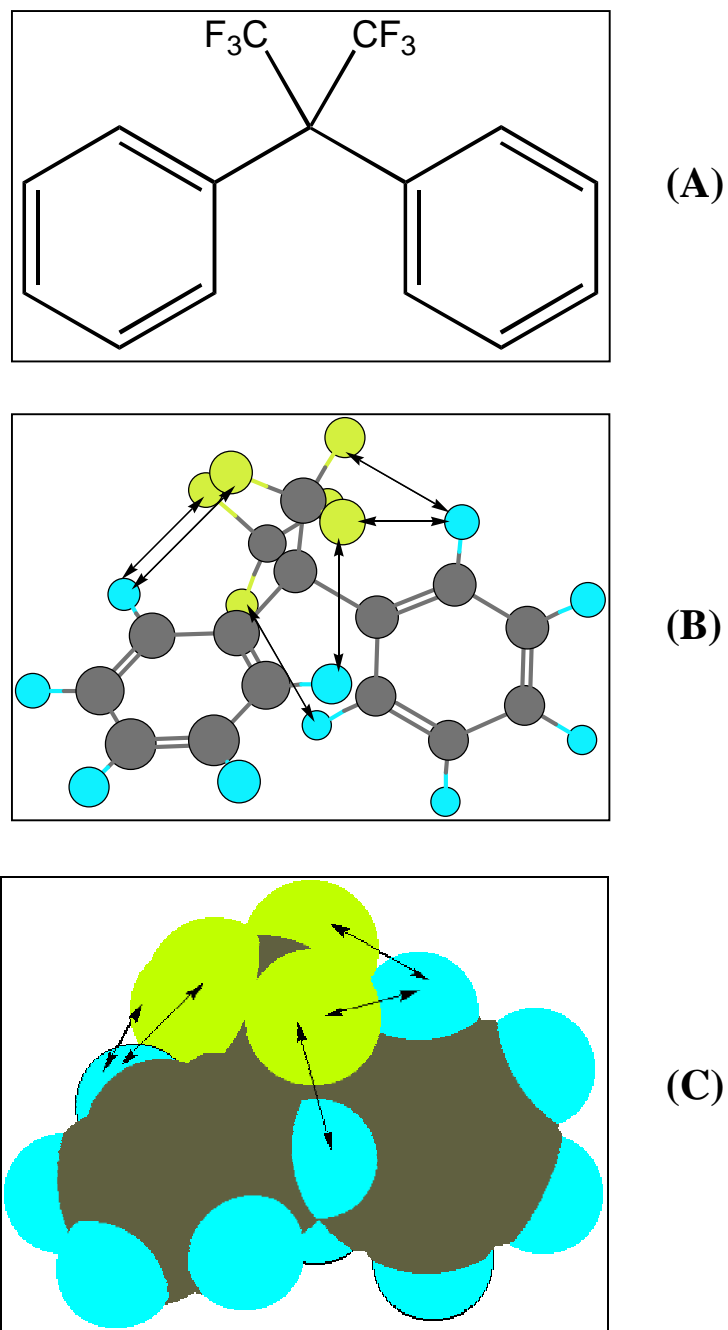
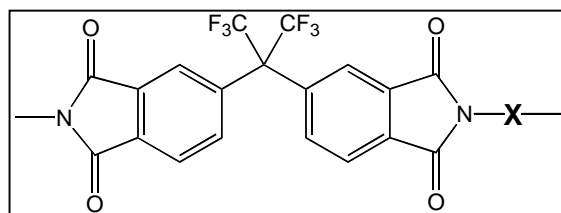


Figure 2.5.1.1 6F Biphenyl Showing Steric Hindrance Between Ph-H's and F's (A) 2-Dimensional (B) 3-Dimensional , Ball and Stick (C) 3-Dimensional, Space Filling



Table 2.5.1.1 Effect of the Structure of Substituted Diamines in 6FDA Polyimides on Glass Transition Temperature, Permeability, Diffusion, and Solubility Coefficient Ratios for the System O<sub>2</sub>/N<sub>2</sub><sup>242</sup>



<b>-X-</b>	<b>T<sub>g</sub> (°C)</b>	<b>P(O<sub>2</sub>) (Ba)</b>	<b>P(O<sub>2</sub>)/P(N<sub>2</sub>)</b>	<b>D(O<sub>2</sub>)/D(N<sub>2</sub>)</b>	<b>S(O<sub>2</sub>)/S(N<sub>2</sub>)</b>
	<b>298</b>	<b>3.0</b>	<b>6.7</b>	<b>5.0</b>	<b>1.3</b>
	<b>335</b>	<b>11.3</b>	<b>5.0</b>	<b>3.9</b>	<b>1.3</b>
	<b>377</b>	<b>109</b>	<b>3.5</b>	<b>2.7</b>	<b>1.3</b>
	<b>351</b>	<b>4.2</b>	<b>5.3</b>	<b>4.3</b>	<b>1.2</b>
	<b>355</b>	<b>13.4</b>	<b>5.0</b>	<b>4.1</b>	<b>1.2</b>
	<b>420</b>	<b>122</b>	<b>3.4</b>	<b>2.8</b>	<b>1.2</b>

Langsam and Burgoyne investigated ortho-alkyl diamines and their effect on restricting the C-N bond rotation (Figure 2.5.1.2).<sup>243</sup> They demonstrated that an *o*-methyl substituted 9,9-bis(4-aminoaryl)fluorene condensed with 6FDA reduced in a 5 fold increase in O<sub>2</sub> permeability while O<sub>2</sub>/N<sub>2</sub> selectivity only decreased by 8%. Polyimides having an ethyl instead of methyl substituent were shown to increase O<sub>2</sub> permeability and restrict rotational freedom, affording higher T<sub>g</sub>s.<sup>243</sup> Each of these observations can be rationalized by the restricting influence of the substituent on the rotational freedom about the imide C-N bond while concomitantly inhibiting intermolecular chain packing.

Several researchers have investigated using sulfone bridging units to achieve high permselectivities.<sup>244-246</sup> Generally, sulfone linkages give high selectivity but low permeability. Kawakami et al.<sup>245</sup> noted possible charge transfer complex formation with sulfones, which usually increases chain packing density and suppresses segmental mobility. The effect of polar substituents such as bromine,<sup>247</sup> chlorine and fluorine<sup>248</sup> have also been investigated. A polar substituent, such as bromine, is known to increase intersegmental attractions, which lead to high diffusive selectivities.<sup>247</sup> Stern et al.<sup>249</sup> recently reported permselectivity characteristics for a select number of 6FDA based polyimides in combination with phenolic containing diamines (Figure 2.5.1.3 and Table 2.5.1.2). In particular, the 6FDA/HAB homopolymer exhibited a considerable improvement in O<sub>2</sub>/N<sub>2</sub> selectivity while maintaining good O<sub>2</sub> permeation.

### 2.5.2 *Meta* versus *Para* Isomers

Several researchers have reported on the differences observed by varying the diamine linkage from *meta* to *para*.<sup>250-253</sup> It has been found that *meta* catenation tends to decrease permeability and increase selectivity due to impeded intra and intersegmental motion. One good comparison is between the two isomers, PMDA-4,4'-ODA (4,4') and PMDA-3,3'-ODA (3,3') shown in Figure 2.5.2.1.<sup>254</sup> The 4,4' system has a T<sub>g</sub> of 400°C compared with that of 280°C for the 3,3'-isomer. Based on this information alone, it may be surmised that the 4,4' isomer would have the lower permeability when compared to 3,3'. However, there may be other thermal transitions which may specifically influence

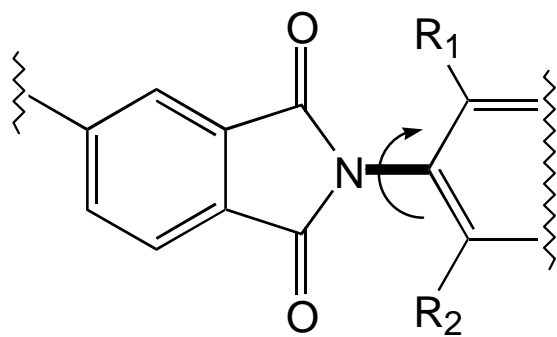


Figure 2.5.1.2 Effects of *ortho*-Substituents on C-N Bond Rotation<sup>243</sup>

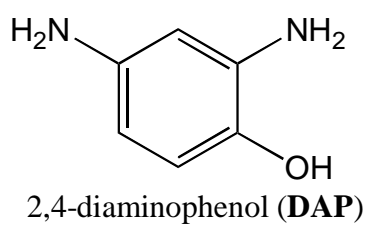
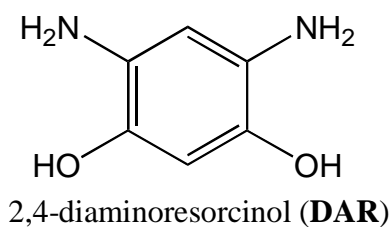
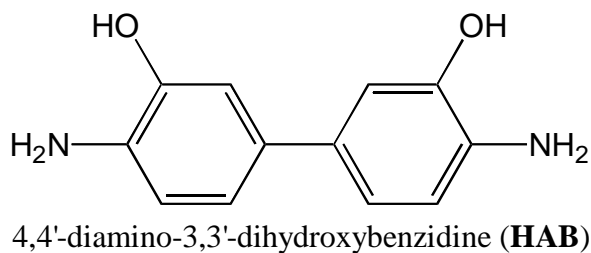


Figure 2.5.1.3 Hydroxyl-containing Diamine Monomers<sup>249</sup>

Table 2.5.1.2 Permeability for Hydroxyl-containing 5,5'-[2,2,2-Trifluoro-1-(trifluoromethyl)ethylidene] bis-1,3-isobenzene-furandione (6FDA) Based Polyimides<sup>249</sup>

System <i>6FDA</i> /	Permeability	
	O(2) (Ba)	O(2)/N(2)
HAB*	1.6	9.3
HAB**	1.8	7.5
DAP	2.4	7.1
DAR	2.2	7.4

\*thermally imidized-insoluble film

\*\*chemically imidized-soluble

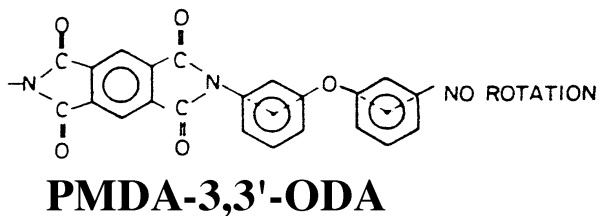
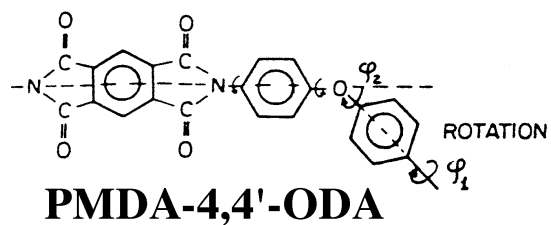


Figure 2.5.2.1 Differences in Intra-segmental (rotational) Mobility of Two Polyimide Isomers: PMDA-4,4'-ODA (*para*-isomer) and PMDA-3,3'-ODA (*meta*-isomer)<sup>254</sup>

Table 2.5.2.1 Effect of Diamine Isomers on Gas Permeability and Selectivity<sup>239</sup>

<i>Isomer</i>	$P(O_2)$ Ba	$P(O_2)/P(N_2)$
PMDA-4,4'-ODA	0.22	4.5
PMDA-3,3'-ODA	0.13	7.2

gas separation characteristics. In fact, the 4,4' is twice as permeable when compared to 3,3' isomer. This is because, unlike the 4,4' species, the 3,3' isomer has no small-scale sub- $T_g$  secondary relaxations due to restricted intrasegmental mobility in the glassy state (Table 2.5.2.1).<sup>239</sup> Figure 2.5.2.1 visually depicts the rotational differences between the 4,4' and the 3,3' isomers.

### 2.5.3 Chemical or Electrostatic Crosslinking, and Annealing

A polymer with the appropriate chemical structure may undergo thermal and/or ultraviolet (UV) promoted crosslinking. Chemical crosslinks, in some cases, may promote an increase in selectivity while only moderately affecting the permeability. Recently, Rezac et al.<sup>255</sup> reported a study of blends utilizing in-chain aliphatic diacetylene-functionalized polyimides with wholly aromatic non-reactive polyimides. Acetylene moieties are known to undergo thermal crosslinking at or above 240°C. The authors report both an increase in O<sub>2</sub> permeability and an increase in O<sub>2</sub>/N<sub>2</sub> selectivity for crosslinked blends. Although they report values of O<sub>2</sub> permeability and O<sub>2</sub>/N<sub>2</sub> selectivity were only 1.30Ba and 6.8, respectively, these might have been increased by employing a better base material in the blends. The base material consisted of 6FDA/bis(4-aminophenyl) isopropylidene. Rezac et al.<sup>256</sup> have also reported on acetylene terminated polyimide/non-reactive polyimide blends which exhibit no appreciable change in permeability or selectivity after cure. The cured blends did show good solvent resistance. Polyarylates have also been investigated for their gas separation characteristics. Those containing in-chain benzocyclobutane units were crosslinked above 180°C.<sup>257</sup> Unfortunately, apparent degradation led to an increase in permeability and a decrease in selectivity; the opposite of what is expected for simple crosslinking.

Ultraviolet irradiation is also known to promote crosslinking. Carbonyl group electrons, eg. in benzophenone, can be excited to a higher energy state when exposed to UV light. In the excited state, carbonyls can abstract labile protons from other species in the system (usually benzylic or methylene protons) to generate carbon based radicals. An intermolecular crosslink is formed when carbon bearing radicals from two chains

combine to form a chemical bond. Kita et al.<sup>258</sup> and others<sup>259-261</sup> have recently reported on UV photocrosslinking of benzophenone containing polymers. Kita et al. reported that as the UV irradiation time was increased, the permeability decreased. The reduction in permeability was shown to be a result of a decrease in the diffusivity coefficient rather than a change in the solubility constant. Overall, impressive permselectivity values were reported (Table 2.5.3.1).

Electrostatic or ionic crosslinks have been explored. Chen et al.<sup>262</sup> reported on a series of polystyrenes with varying sulfonate content. It was observed that as the sulfonate content increased, lower permeabilities and higher selectivities resulted. This phenomenon was interpreted as resulting from electrostatic crosslinking. The selectivity coefficient for these materials varied with the counter ion, eg.  $\text{Na}^+$  or  $\text{Mg}^{2+}$ , with the best combination of  $\text{O}_2/\text{N}_2$  selectivity (11.7) and  $\text{O}_2$  permeability (0.42 Ba) being obtained for  $\text{Mg}^{2+}$  with 27.5 mole percent sulfonation.

Electrostatic crosslinking via polyimides with pendant carboxylic acids<sup>249,263</sup> and sulfonic acids<sup>249</sup> have also been reported. Li et al.<sup>263</sup> have compared polyimides containing 1,3-phenylene diamines with and without a carboxylic acid group in the 5-position. The  $T_g$  of the carboxylic acid containing polyimide was found to increase due to restricted rotation imposed by the bulky group and possible intermolecular electrostatic crosslinking. The fractional free volume of the polymer increased with the acid group and led to a higher permeability coefficient. In addition to a 20% higher  $\text{O}_2$  permeabilities, higher  $\text{O}_2/\text{N}_2$  selectivities were also reported (27%) for the carboxyl functionalized polyimides.

Increased permselectivity can be obtained with polymer membranes containing cobalt complexes due to facilitated transport of molecular oxygen.<sup>264-268</sup> Chen et al.<sup>264</sup> reported the permselectivity behavior of polycarbonate blended with Co(III) acetylacetonate ( $\text{Co}(\text{acac})_3$ ). For the system with 3wt%  $\text{Co}(\text{acac})_3$  there is a 13% loss in  $\text{O}_2$  permeability and a gain of 28% in  $\text{O}_2/\text{N}_2$  selectivity. Even though the reason for this favorable trade-off is not completely understood, it may be related to specific interactions between the carbonyls in the polycarbonate and the cobalt complex which were detectable

Table 2.5.3.1 Permeability coefficients for unirradiated and irradiated polyimide films at 35°C and 2 atm<sup>258</sup>

System	UV exposure Time (min)	Permeability		
		O(2) (Ba)	N(2) (Ba)	O(2)/N(2)
<b>BTDA-TMPD*</b>	0	9.84	1.79	5.5
	1	4.15	0.75	5.3
	10	0.48	0.04	14
	30	0.20	0.02	14
<b>BTDA:6FDA(1:1)/ TMPD</b>	0	12.3	2.73	4.5
	30	1.74	0.18	9.6
	60	1.58	0.15	11

\*TMPD=2,4,6-trimethyl phenylenediamine



by FTIR. Ruan et al.<sup>267</sup> not only report an increase in O<sub>2</sub>/N<sub>2</sub> selectivity but also an increase in O<sub>2</sub> permeability with their cobalt complex/polymer system.